March 6, 1975

To the Graduate Council:

I am submitting herewith a thesis written by Roy Kyle Holbert, Jr., entitled "On the Thermal Cycling of Aluminum Matrix Composite Materials." I recommend that it be accepted in partial fulfillment of the requirements for the degree of Master of Science, with a major in Engineering Science.

Maurice A. Wright, Major Professor

We have read this thesis
and recommend its acceptance:

Walter Frost

N. L. Loeffler

Accepted for the Council:

Hilton A. Smith
Vice Chancellor
Graduate Studies and Research

A

ON THE THERMAL CYCLING OF ALUMINUM MATRIX COMPOSITE MATERIALS

A Thesis

Presented for the

Master of Science

Degree

The University of Tennessee

Roy Kyle Holbert, Jr.

December 1975

1266351

ACKNOWLEDGMENTS

The author wishes to express his sincere appreciation to Dr. M. A. Wright, Professor of Metallurgical Engineering at The University of Tennessee Space Institute, for his counsel, instruction, and encouragement throughout the course of this study and investigation.

The author is grateful to J. Goodman and R. Harney for their technical help and advice. The author also appreciates the cooperation, help, and discussion of his colleagues at The University of Tennessee Space Institute Materials Laboratory throughout this research. They are: F. Iannuzzi, H. Kulkarni, M. White, E. Flowers, and V. Liu.

The author also wishes to thank Dr. B. H. Goethert, Dean Emeritus of The University of Tennessee Space Institute, and the Department of the Navy, Washington, D. C., for the opportunity to conduct this investigation.

The author would like to express his appreciation to his wife, Emily, for her assistance in editing this thesis and for her reassurance during its writing.

ABSTRACT

Various 6061 aluminum matrix composite materials were thermally cycled from room temperature to 425°C. The materials were reinforced with stainless steel, silicon carbide, and boron fibers. The mechanical properties that were investigated included longitudinal and transverse modulus, longitudinal and transverse ultimate tensile strength, Poisson's ratio, and density. The total heating and cooling cyclic period was varied from three to six to twelve minutes per cycle, and then the room temperature mechanical properties were compared to those obtained from the as-received material. The thermal expansion of the boron-aluminum composite was measured during the thermal cycling process for each of the cyclic periods.

It was observed that the matrix sustained damage during the thermal cycling in all of the materials. The damage was in the form of cracks and voids. The matrix damage increased with cyclic period. There was degradation in the tensile and transverse strength for all of the thermally cycled materials. The degradation of the composite strength was more severe in the boron-aluminum material than in the other materials investigated. The strength reduction in boron-aluminum became more pronounced as the cyclic period increased. The elastic modulus of some of the thermally cycled material decreased. Metallographic

observations of thermally fatigued material produced evidence of grain boundary movement. The thermal expansion results indicated that by increasing the cyclic period, the maximum extension during one cycle decreased.

The results of the investigation of the composites' strengths were explained in terms of the degradation of the fiber-matrix bond. Since a unique strength value cannot be assigned to the brittle boron and silicon carbide fibers, the theoretical prediction of the tensile strength of the composite reinforced with these fibers was discussed using a range of values defined by an upper and lower strength limit. The lower limit was predicted from a model with a weak interfacial bond, and a strong bond was assumed in calculating an upper limit. It was concluded that the thermal cycling process deteriorated the fiber-matrix bond.

The extension of the boron-aluminum material during thermal cycling was observed to be controlled by the matrix at the lower temperatures during the thermal fatigue process. As the temperature increased, the stresses acting on the fibers due to the greater thermal expansion of the matrix were reduced. As the cyclic period increased, the stresses acting on the fibers were relaxed, and the thermal expansion of the composite was dominated by the thermal expansion of the fiber.

TABLE OF CONTENTS

CHAPTER		PAGE
I.	INTRODUCTION	1
II.	REVIEW OF LITERATURE	3
	Introduction	3
	Interfacial Bond	3
	Theoretical Composite Strengths	15
	Thermal Stresses	19
	Thermal Cycling	21
	Thermal Expansion of Composites	27
	Creep of Composites	31
III.	EXPERIMENTAL PROCEDURE	37
	Test Material	37
	Mechanical Property Determination	38
	Thermal Cycling Furnaces	39
	Dilatometer	40
	Density Tests	43
	Errors	44
IV.	RESULTS	50
	Ultimate Tensile Strengths	50
	Stainless steel-aluminum composites	50
	Silicon carbide-aluminum composites	51
	Boron-aluminum composites	52
	Elastic Modulus, Density, and Poisson's Ratio	53

CHAPTER PAGE

Thermal Expansion During Cycling 54

Metallographic and General Observations. . . . 57

V. DISCUSSION 60

Theoretical Ultimate Tensile Strengths of Unidirectional Composites. 60

Brittle fibers 60

Ductile fibers 65

Degradation of the Fiber-Matrix Bond 65

Effect of Thermal Cycling on Elastic Modulus. 70

Cracks and Voids in the Matrix 71

Thermal Expansion of Composites During Thermal Cycling. 73

VI. CONCLUSIONS. 77

VII. RECOMMENDATIONS. 79

BIBLIOGRAPHY 80

APPENDIX 87

VITA 128

LIST OF TABLES

TABLE		PAGE
I.	The Effect of Thermal Cycling on Mechanical Properties of Stainless Steel Reinforced Aluminum Alloy.	88
II.	The Effect of Thermal Cycling on Mechanical Properties of Silicon-Carbide Reinforced Aluminum Alloy.	89
III.	The Effect of Thermal Cycling on Mechanical Properties of Unidirectional Boron Reinforced Aluminum Alloy	90
IV.	The Effect of Thermal Cycling on Mechanical Properties of 0° to 90° Crossplied Boron Reinforced Aluminum Alloy	91
V.	The Effect of Thermal Cycling on Mechanical Properties of ±45° Crossplied Boron Reinforced Aluminum Alloy	92
VI.	The Relative Thermal Expansion of a Boron-Aluminum Composite Subjected to Thermal Cycling Using a Three-Minute Period	93
VII.	The Relative Thermal Expansion of a Boron-Aluminum Composite Subjected to Thermal Cycling Using a Six-Minute Period	94

TABLE PAGE

VIII. The Relative Thermal Expansion of a Boron-Aluminum Composite Subjected to Thermal Cycling Using a Twelve-Minute Period. 96

IX. The Theoretical and Experimental Composite Strength as Obtained for As-Received and Thermally Cycled Material 100

X. The Experimentally Determined Number of Fibers in a Composite 101

XI. The Theoretical Composite Strength as Obtained for As-Received and Thermally Cycled Stainless Steel Reinforced Material. . 102

LIST OF FIGURES

FIGURE		PAGE
1.	A Diagram of the Placement of a Composite Specimen into the Dilatometer	103
2.	The Calibration Curve of the LVDT in the Thermal Expansion Measurement System.	104
3.	The Temperature Changes with Time for Specimens Subjected to Thermal Fatigue in the Dilatometer	105
4.	The Surface of Unidirectionally Reinforced Boron-Aluminum After Exposure to 6,000 Cycles, 20°C to 425°C, Three Minutes per Cycle; X 193	106
5.	The Surface of Unidirectionally Reinforced Boron-Aluminum After Exposure to 6,000 Cycles, 20°C to 425°C, Twelve Minutes per Cycle	107
6.	A Scanning Electron Micrograph Showing Extensive Surface Disruption Resulting from Thermal Cycling Using a Twelve-Minute Period; X 100	108
7.	A Scanning Electron Micrograph Showing Apparent Grain Boundary Process; X 1,000. . . .	109

FIGURE PAGE

8. The Surface of Unidirectionally Reinforced Silicon Carbide-Aluminum After Exposure to 6,000 Cycles, 20°C to 425°C, Three Minutes per Cycle; X 193. 110

9. The Surface of Unidirectionally Reinforced Silicon Carbide-Aluminum After Exposure to 6,000 Cycles, 20°C to 425°C, Six Minutes per Cycle; X 193. 111

10. The Surface of Unidirectionally Reinforced Silicon Carbide-Aluminum After Exposure to 6,000 Cycles, 20°C to 425°C, Twelve Minutes per Cycle; X 193. 112

11. The Surface of Unidirectionally Reinforced Stainless Steel-Aluminum After Exposure to 6,000 Cycles, 20°C to 365°C, Three Minutes per Cycle; X 193. 113

12. The Surface of Unidirectionally Reinforced Stainless Steel-Aluminum After Exposure to 6,000 Cycles, 20°C to 365°C, Six Minutes per Cycle; X 193. 114

13. The Surface of Unidirectionally Reinforced Stainless Steel-Aluminum After Exposure to 6,000 Cycles, 20°C to 365°C, Twelve Minutes per Cycle; X 193. 115

FIGURE PAGE

14. The Surface of a Boron Reinforced Specimen Subjected to Five Cyclic Temperature Changes, 20°C to 425°C, Six Minutes per Cycle. 116

15. The Internal Voids in a Boron Reinforced Specimen Subjected to 6,000 Thermal Cycles; X 193 117

16. The Thermal Expansion of Boron-Aluminum During the Tenth to Twentieth Thermal Cycles. 118

17. The Thermal Expansion of Boron-Aluminum During the Fiftieth to One Hundredth Thermal Cycles. 119

18. The Thermal Expansion of Boron-Aluminum During the Four Hundredth to Six Hundredth Thermal Cycles. 120

19. The Thermal Expansion of Boron-Aluminum During the One Thousandth to Fourteen Hundredth Thermal Cycles 121

20. The Thermal Expansion of Boron-Aluminum During the Two Thousandth to Twenty-two Hundredth Thermal Cycles. 122

21. The Thermal Expansion of Boron-Aluminum During the Four Thousandth to Forty-ninth Hundredth Thermal Cycles. 123

FIGURE PAGE

22. The Thermal Expansion of Boron-Aluminum During the Six Thousandth Thermal Cycle 124

23. The Thermal Expansion of Boron-Aluminum Cycled with the Three-Minute Period 125

24. The Thermal Expansion of Boron-Aluminum Cycled with the Six-Minute Period 126

25. The Thermal Expansion of Boron-Aluminum Cycled with the Twelve-Minute Period. 127

CHAPTER I

INTRODUCTION

During the service life of many materials, there are applications that subject the material to cyclic temperature changes. This temperature variation can possibly shorten the material's service life many times by a considerable amount. Knowledge of the degree of degradation is needed by the design engineers in order to assign structural limitations to the material to avoid premature failure.

The purpose of this investigation was to help determine the design limitations that should be set on aluminum matrix composite materials that are subjected to thermal cycling. The materials which were investigated were reinforced with boron, silicon carbide, and stainless steel fibers. These materials were susceptible to thermal fatigue because of the difference in the thermal expansion coefficients of the components.

The use of these materials is destined to become a necessity in the coming years, especially in aerospace application. These materials are constructed with high strength, high stiffness, and low density fibers embedded in a ductile metal matrix. Their specific mechanical properties are usually much higher than common aerospace

material. Therefore, the use of these composites would result in weight savings which would increase the potential pay-load of an aerospace vehicle.

The use of these composites is not limited just to aerospace applications. Their use is needed in any weight critical applications such as automobiles, trucks, ships, and many other passenger and cargo transport vehicles.

Since many parts of these transport vehicles may be subjected to thermal variation, this investigation can be considered a worthwhile project because these parts could be constructed from metal matrix materials in the near future.

CHAPTER II

REVIEW OF LITERATURE

A. INTRODUCTION

In order to set design limitations on aluminum matrix composites that are exposed to repeated temperature variations during service, the amount of possible degradation in strength of a composite becomes relevant. To understand the decline of strength of the material during the temperature changes leads to a study of the thermal cycling investigative process. This, in turn, leads to a discussion of the thermal expansion and creep of a composite. The current work done in these areas will be reported in this chapter.

The first part of the review will concern the bonding of the matrix to the fiber. This bond effects the load carrying capabilities of the composite; therefore, making it a logical suspect for any strength degradation.

B. INTERFACIAL BOND

The following definition of an interface was proposed by Metcalfe [1]:[1] "An interface is the region of significantly changed chemical composition that constitutes

---

[1]Numbers in brackets refer to similarly numbered references in the bibliography.

the bond between the matrix and reinforcement for transfer of loads between these members of the composite structure." Also, the interface must not degrade the strength of the filament. The ideal interface is one in which there is no chemical interdiffusion between the two components of the composite.

The composites that are fabricated by diffusion bonding, appear free of chemical interaction after fabrication. This group includes aluminum-boron, aluminum-stainless steel, and aluminum-silicon carbide. The thermodynamic data show that the components should react, and they do, when the aluminum melts. However, if the optimum processing is used, the reaction is negligible [1].

For the bonding between the aluminum matrix and the filaments of boron or silicon carbide, Metcalfe [1] has reported that the characteristics of these bonds can be explained in terms of a bond between the aluminum oxide film and either the oxide film on the boron or the silicon oxide film on the silicon carbide. However, more work has been suggested for the silicon-carbide reinforcement. In the case of boron fibers, the oxide film bond would explain the stability when in contact with aluminum because ordinarily these elements are highly reactive with each other. Evidence of this type of bond was presented by Klein and Metcalfe [2] based on the extraction of the oxide film. In work done by Midwest Research Institute [3], aluminum oxide (Al_2O_3) was

identified in the interface region of a section of 6061 aluminum-45% boron composite. It was concluded that no boron oxides were found because they would have been reduced by reaction with the aluminum matrix. After annealing, aluminum diboride was found in reaction zones.

Chemical reaction between the fiber and matrix begins when the oxide films break down. In a boron-aluminum system this reaction results in the formation of aluminum diboride. Reactions of this type in small isolated areas of the interface seem to strengthen the bond to obtain the maximum tensile strength. But when a boron filament becomes surrounded by a thick layer of aluminum diboride, the composite shows a strength degradation according to the results of Klein and Metcalfe [2] which will be discussed later.

Disruption of the oxide film can be caused by mechanical shear at the interface and spheroidization at high temperatures [1]. Ebert and Wright [3] have reported that an aluminum-50% boron composite will have an increase of 250 pounds per square inch (psi) of stress on the matrix when the temperature is dropped by 1°F. Therefore, in the cooling part of the diffusion bonding process, the stress developed on the matrix should exceed the yield point and plastic deformation should result. Also, during the heating part of the process, force is applied in order to increase contact of the two materials when the matrix deforms

plastically. The plastic deformation that occurs during these heating and cooling phases may lead to mechanical shear which would lead to the disruption of the oxide film. However, this oxide film breakdown occurs only at local sites. Shear would also explain the damaging effect that high pressures have in hot processing of aluminum matrix material.

The second method of interfacial breakdown is by spheroidization. This is when the oxides of the matrix and fiber tend to group to form small sphere-like particles. Since the oxide films have high surface energies, they are unstable; therefore, prolonged time at high temperatures or excessive temperatures lead to spheroidization of the films [4].

Antony and Chang [5] observed both a composite and a fiber strength degradation when an aluminum-27% boron composite was thermally cycled between room temperature and 800°F for 100 cycles. The authors concluded that the composite strength decrease is adequately accounted for by the degradation in the boron filaments without any reaction to the filament-matrix bond. However, they also report that fiber degradation is caused by undefined changes in structure and/or residual stress distribution within the filament.

Stuhrke [6] reported a decrease in strength with boron-aluminum composites when left at temperatures of 450, 700, and 1,000°F. He concluded that there were two reasons

for this reaction. First, the thermal annealing led to the uncoupling of the fiber and matrix. Second, the interaction of the boron with the aluminum caused degradation leading to a reduction in the strain to failure.

Kreider, Dardi, and Prewo [7] reported that boron-aluminum material showed a 12% strength reduction after being exposed to a temperature of 700°F in air for 1,000 hours.

Metcalfe [4] believes that these investigative results can be explained in terms of the fiber degradation caused by reaction between fiber and matrix. His belief is supported by the recent results of Klein and Metcalfe [8] of the breakdown of the interface of boron-aluminum composites at temperatures above 700°F.

Weight and Intwala [9] reported a strength reduction in boron-aluminum composites when heated for four hours at 600°C. It was concluded that this strength degradation resulted from the strength reduction of the fiber and that the bond between the matrix and fiber appeared to be degraded by the heat-treatment.

In the thermal cycling from room temperature to 425°C of three different aluminum matrices (1100, 2024, and 6061) reinforced with boron fibers, the strengths degraded after 6,000 cycles toward a theoretical lower bound. This limit was derived by assuming that no bond existed between fiber and matrix. This effect was reported by Wright and Wills [10]. They concluded that the decrease in the

composite strength resulted from the degradation of the strength of the fiber-matrix bond.

Pattnaik and Lawley [11] noticed that after heat treating high purity aluminum composites reinforced with stainless steel fiber, a reaction between the fiber and the matrix occurred. In the as-received condition, there were isolated reacted areas similar to those observed in the boron-aluminum composites.

Baker [12] concluded in his studies of stainless steel aluminum that the best fatigue performance occurred in slightly reacted composites. However, Pinnel and Lawley [13] reported that optimum properties were obtained from composites which were, for the most part, free of reaction.

Pattnaik and Lawley [11] observed that the product of the reaction between the stainless steel and the aluminum matrix consisted of an iron alumide phase. In heat treating, the reaction resulted in the formation of a "corncob" structure on the surface of the reinforcement. The reaction was not uniform over the fiber length. It was noted by the authors that the reaction occurred in an irregular radial pattern similar to that which was reported by Metcalfe [4] for the boron-aluminum system.

Baker observed local breakdown of the matrix-aluminum bond. He concluded that a protective film existed between the fiber and the matrix.

Jones [14] reported that the stainless steel-aluminum bond is basically mechanical. He drew his conclusion from the clean separation of the fiber from the matrix that occurred in a tensile test. Metcalfe and Klein [15] proposed that this clean separation would also be expected if the fiber-matrix bond was formed between the oxides that existed on the surface of the two components of the composite. The effect of elevated temperature on aluminum-stainless steel composites was reported by Pattnaik and Lawley [16]. The results show that the strengths of the fibers decreased with increased exposure to high temperature. Forrest and Christian [17] measured the shear and transverse strength of 6061 aluminum reinforced with uncoated boron fibers, silicon carbide coated boron fibers, and boron nitride coated boron fibers. They concluded that the standard 6061 uncoated boron composite which was solution heat treated at 980°F followed by aging, gave the most desirable mechanical properties. The composites that contained coated boron fibers were shown to reduce the reaction with the aluminum matrix.

Kreider, Dardi, and Prewo [7] reported that aluminum reinforced with 0.0042-inch-diameter boron fibers showed no change in strength when aged at 700°F for 1,000 hours as previously reported. Severe reaction of these aluminum matrices with the various fibers lowers the tensile strength of the composite. If the reaction is extremely

severe, debonding may occur. The strengths of the fibers are also degraded by the reaction.

Klein and Metcalfe [2] reported that the composites show a decrease in tensile strength when aluminum diboride covers the surface of the boron fibers. Their experiment consisted of leaving boron-aluminum specimens at 940°F for different periods of time. The strength of both the composites decreased as the time-at-temperature increased. The authors extracted fibers from composites that had been subjected to the high temperature environment for 165 hours. The strength of the fibers had decreased appreciably. The aluminum diboride layer was removed from the fiber surface with red fuming nitric acid and the resulting fibers were pulled. The subsequent strengths increased within 93% of their original strength. Therefore, it was concluded that the reaction of the aluminum with the boron was the primary cause of the strength degradation. Metallophic observations indicated that the aluminum diboride film was extensively cracked. The presence of these cracks was assumed to be responsible for the strength degradation.

Pattnaik and Lawley [16] reported that the strength reduction in the aluminum-stainless steel composites was due to the premature cracking in the interface reaction zone. They also noted that any reaction tended to produce voids or holes by a process that they considered similar to the

Kirkendall effect. In contrast, when these components react, the reported holes that form at the interface between the aluminum matrix and boron fibers are considered to be responsible for the 20% contraction that occurs with the formation of aluminum diboride [2, 7].

One method of testing the strength of the bond that exists between the reinforcement and matrix is by determining the transverse strength of the composite. The present theories of transverse strength establish an upper and lower limit. The upper limit corresponds to that which would result from a strong interfacial bond while the lower limit is associated with a weak bond.

A theory for predicting the transverse strength has been proposed by Chen and Lin [18]. They employed a finite-element method to determine the normalized distortional energy at selected points throughout the composite. Then they utilized the von Mises-Hencky criterion to determine the probability of local failure. Failure was assumed to occur when the distortional energy present in the composite exceeded a critical energy value. Thus the transverse strength of the composite was determined using the following equation:

$$S_i = S_m \, \bar{\sigma}_c / (U_{max})^{1/2} \, , \qquad (1)$$

where

S_i = the transverse strength,

S_m = the strength of the matrix,

$\bar{\sigma}_c$ = the applied stress on the composite as determined by the finite-element method,

U_{max} = the maximum normalized distortional using $\bar{\sigma}_c$.

Both $\bar{\sigma}_c$ and U_{max} are functions of fiber volume content, fiber array, conditions of fiber-matrix bond, and constituent properties. The authors used two types of metal matrix composites to verify experimentally their results. They derived theoretically with Equation (1) the upper and lower limits using a square and hexagonal array of fibers for the material, 6061 aluminum-boron and 2024 aluminum-stainless steel. As can be observed from inspection of Equation (1), the transverse strength is not expected to exceed the matrix strength. The results that were obtained suggested that the boron-aluminum material was a perfectly bonded square array of fibers and the stainless steel was a totally debonded hexagonal fiber arrangement.

Adams [19] applied an elastic-plastic analysis to define the transverse strengths of a composite. He indicated that the transverse strengths of boron-aluminum

would be of the same order as the bulk matrix tensile strength. He did not account for the strengths of the interface or for the transverse strengths of the filament. Theoretically, if these are known, plus the properties of the matrix, the failure mode could be predicted.

An alternative method for calculating the lower limit of the transverse strengths has been suggested by Cooper and Kelly [20]. Essentially the fibers in the composite are assumed to be replaced by holes. Then the equation used to calculate the transverse strength is:

$$\sigma_t = \sigma_m(1 - \sqrt{\frac{4V_f}{\pi}}) \quad , \tag{2}$$

where

σ_t = the transverse strength,

σ_m = the matrix strength,

V_f = the volume fraction.

When the interface strength is greater than zero but less than the strength of the matrix, Equation (2) is altered to be:

$$\sigma_t = \sigma_m(1 - \sqrt{\frac{4V_f}{\pi}}) + \sigma_i'(\sqrt{\frac{4V_f}{\pi}}) \quad , \tag{3}$$

where

σ_i' = the average transverse stress required to induce interface failure.

The upper limit was predicted to be the plain strain strength of the matrix which was about 1.15 times the bulk matrix strength.

According to Klein and Metcalfe [2], failure of well bonded boron-aluminum material takes place in the matrix or in splitting of the 0.0042-inch-diameter fiber. The as-received specimen they tested failed at the interface, indicating a less than perfect bond. In heat treating at 1,000°F for times up to one hour, the failure occurred in the matrix, indicating a strengthened interface. Longer times at the same temperature reduced the tensile transverse strength with failure occurring by the fiber splitting (two to five hours) or at the interface (over five hours). The reason advanced for the reduction in transverse strength was associated with the generation of internal stresses and porosity due to the 20% volume contraction that takes place with the formation of aluminum diboride.

Paton and Lockhart [21] studied the effect of the formation of iron aluminide on the transverse strengths of aluminum-stainless steel. The bond strength increased with the start of the reaction. But with extensive reaction the

transverse strength decreased because of the brittleness of the reacted interface.

C. THEORETICAL COMPOSITE STRENGTHS

The theoretical ultimate tensile strength of a composite is given by the "Rule of Mixtures" as discussed by Kelly [22]:

$$\sigma_c = V_m\sigma_m + V_f\sigma_f \ , \qquad (4)$$

where

σ_c = the strength of the composite,

σ_m = the strength of the matrix,

σ_f = the strength of the fibers,

V_f = volume percent of the fibers,

V_m = volume percent of the matrix, $(1-V_f)$.

Equation (4) can also be used to describe the strength of a composite reinforced with fibers that exhibit a scatter in their strength values. However, unique strength of brittle fibers cannot be calculated because the strength of the fiber is length dependent and tends to obey a Weibull distribution as reported by Daniels [23] and Coleman [24]. Corten [25] has suggested that the probability, $G(\sigma)$, of a fiber failing under a stress, σ, can be given by the equation:

$$G(\sigma) = 1 - \exp\left[-\frac{L}{d}\left(\frac{\sigma-\sigma_*}{\sigma_o}\right)^{\omega}\right] , \qquad (5)$$

where

L = length of fiber,

d = diameter of fiber,

σ_* = lower limiting strength, when $G(\sigma) = o$,

σ_o = distribution scale factor

ω = distribution shape factor used to describe scatter of data.

For simplicity, σ_* is taken to be zero. When the equation is algebraically rearranged to the form of

$$\ell n\ \ell n\left[\frac{1}{1-G(\sigma)}\right] = \omega[\ell n\ \sigma - \ell n\ \sigma_o] + \ell n\ \frac{L}{d} , \qquad (6)$$

ω and σ_o can be found experimentally.

Using the theories of Daniels [23] and Coleman [24], the mean strength, σ_B , of a bundle of brittle fibers can be determined using the equation:

$$\sigma_B = \sigma_o\left(\frac{L}{d}\ \omega e\right)^{-1/\omega} . \qquad (7)$$

The lower bound strength of a composite reinforced with brittle fibers can be assumed to be related to the strength of a bundle with a length equal to the gage length of the specimen. If the matrix is effectively assumed to

carry no load and does not transfer any stress to that of a simple bundle, then the lower bound strength of the composite can be predicted from the Rule of Mixtures using the equation:

$$\sigma_c = V_f \sigma_B \ . \tag{8}$$

An upper bound strength can be determined by utilizing the cumulative damage theory developed by Rosen [26, 27, 28, 29]. His model for the composite system can be considered to be a series of layers of an "ineffective" length. This length is a reduction of the effective length of a fiber bundle due to the contribution of the matrix. The section of fiber within a layer may be considered as a link in a chain which composes the whole fiber. Then each layer can be considered as a bundle of these links. The composite is made up of a series of bundles. When one of the bundles fails, the composite fails. The ineffective length is extremely small.

Using Equation (7) and substituting the ineffective length, δ, for L, the strength of a bundle of fibers of length, δ, is given by the equation:

$$\sigma_B = \sigma_o \left(\frac{\delta}{d}\, \omega e\right)^{-1/\omega} \ , \tag{9}$$

if ω and σ_o are not length dependent.

Substituting Equation (9) into the Rule of Mixtures enables an expression for the upper bound strength

of a composite to be derived using the equation:

$$\sigma_c = V_f \sigma_o \left(\frac{\delta}{d}\, \omega e\right)^{-1/\omega} + (1-V_f)\sigma_m \ . \qquad (10)$$

If the matrix is elastic, then σ_m can be calculated using Hooke's Law. If the matrix is elastic-plastic, that is, behaves as a real material then the matrix strength, σ_m , will equal its yield strength.

Rosen [28] and Kelly [22] used a shear lag analysis to derive an expression for the ineffective length of fibers present in an elastic-plastic material:

$$\delta = \frac{\sigma_d}{2\tau} \ , \qquad (11)$$

where

σ = the stress in fiber,

τ = the shear yield strength of the matrix,

d = fiber diameter.

In this model, the tensile strength of the fiber will be equal to the bundle strength given by Equation (9). It is to be noted that the ineffective length and the bundle strength are dependent. Therefore, in determining the upper bound strength of the composite, the ineffective length and the upper bound strength have to be calculated iteratively until the values obtained satisfy simultaneously Equations (10) and (11).

D. THERMAL STRESSES

As has been referred to previously, Ebert and Wright [3] reported that a boron-aluminum composite will probably have residual stresses as a result of cooling from the fabrication temperatures. These stresses resulted from the difference in the thermal contraction of the aluminum matrix and the boron fibers. Since the thermal expansion coefficients of silicon-carbide is 4.9×10^{-6} inch/inch/°C, and of stainless steel is 28.9×10^{-6} inch/inch/°C which are larger than the thermal expansion of aluminum, residual stress would be expected to occur in composites with these materials, as reported by Bolz [30].

An analysis of a composite subject to temperature change is reported by Wills [31]. Assuming perfect bonding, the strain of the fiber equals the strain of the matrix. Thus,

$$\alpha_m \Delta T + \varepsilon_m = \alpha_f \Delta T + \varepsilon_f \ , \tag{12}$$

where

α_m = the thermal expansion of the matrix,

ΔT = the temperature range,

ε_m = the strain of matrix due to stresses placed on it by the fiber

$$= \frac{\sigma_m}{E_m} \ ,$$

α_f = the thermal expansion of the fiber,

ε_f = the strain of fiber due to stresses placed on it by the matrix

$= \frac{\sigma_f}{E_f}$.

If there are no external forces on the composite, then the Rule of Mixtures equation describes the equilibrium state of stress, that is:

$$\sigma_f V_f = \sigma_m V_m = o \ ,$$

or

$$\sigma_f V_f = \sigma_m (1-V_f) \ , \tag{13}$$

where

σ_f = the stress on the fiber,

V_f = the volume percent of the fiber,

V_m = the volume percent of the matrix,

σ_m = the stress on the matrix.

By substituting Equation (13) into Equation (12), the elastic stress in the matrix is given by the equation:

$$\sigma_m = - \frac{(\alpha_m - \alpha_f)\Delta T \ E_f E_m V_f}{E_f V_f + E_m (1-V_f)} \ . \tag{14}$$

Therefore, the elastic stress in the fiber is given by the equation:

$$\sigma_f = \frac{(\alpha_m - \alpha_f)\Delta T \; E_f E_m (1-V_f)}{E_f V_f + E_m (1-V_f)} \; . \qquad (15)$$

In 50 volume percent boron-aluminum materials, the magnitude of the elastic stress generated in the matrix when the composite is cooled from a fabrication temperature of approximately 500°C is about 82 ksi. For the 50 volume percent stainless steel these values are larger than the yield stress of 6061 aluminum; and therefore, plastic flow would be expected. At room temperature the aluminum matrix materials are expected to contain residual stresses that would be at least equal to the yield point of the matrix. It is obvious that a large cyclic variation of temperature will result in local yielding of the matrix.

E. THERMAL CYCLING

As a model of thermal fatigue, consider a metal rod constrained at both ends so that its length remains constant during temperature excursions. Also, that material from which the rod is made behaves in an ideally elastic-plastic manner, that is, its stress-strain curve consists of a straight line until the stress value reaches a critical value after which unlimited plastic flow occurs at a constant stress.

If a small temperature change occurs, the constrained thermal expansion will result in the generation of elastic stresses. However, if the temperature variation is large, then plastic flow will be expected to occur. Reversed plastic strain will be obtained on subsequent cooling. If cyclic temperature variations take place, then every cycle will induce equal amounts of plastic flow.

Just how many cycles of this type the material stands before it eventually fails is dependent on the temperature gradient, temperature limit holding times, heating and cooling rates, and the elastic and plastic properties of the phases [31].

In some engineering materials that are subjected to large repeated temperature changes, the differential stresses that result are often high enough to cause local plastic deformation. Sometimes these materials exhibit premature failure and cracks develop that are characteristic of a fatigue process. Thus, because of the thermal gradient, the process of repeated temperature variations is called thermal fatigue. The term is often misleading because at useful service temperatures, creep relaxation is probably the dominant process [32].

Taira [33, 34] has proposed that the damage sustained as a result of a thermal fatigue process can be related to mechanical fatigue providing moderate temperature changes are considered. The stresses in the thermally

fatigued material can be considered to be thermally induced. The damage that is found in these thermally fatigued materials can be attributed to reversed localized deformation.

Higher peak temperatures, the cracking and premature failure that occurs in many engineering materials may be traced to a combination of fatigue and creep. Creep was shown by McClintock and Argon [35] to be accelerated by a thermal fatigue process.

In this paper, the term thermal fatigue is used to describe all processes that produce damage in a specimen subjected to cyclic temperature variations.

Kreider, Dardi, and Prewo [7] investigated the thermal cycling of 6061 aluminum reinforced with 50 volume percent silicon carbide coated boron fibers (Borsic). In their experiments the temperature varied between 70 and 670°F. Their results indicated that width of the unidirectional material increased by about 4% after 5,000 cycles. Extensive surface deformation and protrusions accompanied the change in dimensions. The authors suggested that the density decrease that was also reported resulted from the formation of cracks and voids in the matrix. Metallographic observations of the specimens confirmed the presence of the voids. The flexural strength of most specimens decreased by about 13% after 5,000 cycles. The

strength loss, void formation, and dimensional change increased with increased cycling.

The same authors concluded that the void formation reflected fatigue damage that arose from the cyclic plastic strain resulting from each temperature cycle. The analysis they offered assumed that the matrix was perfectly plastic, and that the fibers were infinitely stiff relative to the matrix. The matrix strain, ε_m , occurring during a temperature change was then described by the equation:

$$\varepsilon_m = (\alpha_m - \alpha_f)\Delta T \ , \tag{16}$$

where

α_m = the thermal expansion coefficient of the matrix,

α_f = the thermal expansion coefficient of the fiber,

ΔT = the temperature change.

In discussing their results, they used the Manson-Coffin law which states that the fatigue life is dependent on the cyclic plastic strain range and is approximated by the equation:

$$\Delta\varepsilon_{pl} = (N/D)^{-0.6} \ , \tag{17}$$

where

$\Delta\varepsilon_{pl}$ = the cyclic plastic strain,

N = the number of cycles to failure,

D = a ductility parameter

= $\ell n(1/1-RA)$,

RA = the fractional reduction of the area in a tensile test.

For a complete temperature reversal, the cyclic plastic strain is equal to twice the matrix strain ($\Delta\varepsilon_{pl} = 2\varepsilon$). Combining Equations (16) and (17) gives:

$$N = \frac{\ell n(1/1-RA)}{[2(\alpha_m-\alpha_f)\Delta T]^{1.6}} . \qquad (18)$$

According to Equation (18) the thermal fatigue life can be increased by increasing the matrix ductility, decreasing the temperature range, and decreasing the difference between the thermal expansion coefficients. However, this analysis does not allow for recovery effects, elastic strain components, or creep. It also assumes that failure will occur at the condition of maximum thermal stress and minimum ductility.

As previously mentioned, Antony and Chang [5], and Wright and Wills [10], reported a strength degradation when boron-aluminum composites were thermally cycled. In addition, Wright [37] reported that cracks developed in the

surfaces of three different types of aluminum matrix material reinforced with boron fibers when these specimens were subjected to excessive cyclic temperature changes. It was concluded that the presence of these cracks reduced the maximum strength of the material. This surface damage was greatest for a 2024 aluminum-boron material. Progressively smaller degrees of damage were observed for composites fabricated using a 6061 aluminum matrix or an 1100 aluminum matrix, respectively. It was concluded that the extent of the degradation of the mechanical properties resulted from the difference in the strength of the fiber-matrix bonds.

Shahanian [38] studied the effect of thermally cycling 2024 aluminum-boron material, 6061 aluminum-boron material, and 6061 aluminum material reinforced with silicon carbide coated boron. Different specimens were cycled from near room temperature to 300 or 500°C. The 2024 aluminum matrix and the 6061 aluminum reinforced with boron exhibited surface "roughing" which was more extensive in the 2024 aluminum matrix. The surface of both matrices developed surface cracks that exposed the fiber. Cracks appeared internally only in the 6061 aluminum matrix. The internal cracks were usually normal to the filament axis. The strength of specimens decreased after thermally cycling for 2,000 cycles with the maximum cyclic temperatures of 300 and 500°C. The specimens cycled with a maximum cyclic temperature of 500°C showed more reduction in strength than those

which were cycled with a maximum cyclic temperature of 300°C. Most of the thermally fatigued specimens were cycled using a cyclic period of three minutes. However, the period was decreased to one minute per cycle for one of the 6061 aluminum-boron specimens. The resulting tensile strength of this specimen was 10% more than that of a similar specimen subjected to the same number of cycles using a three-minute period.

The same author investigated the effect of thermal cycling the boron-aluminum material between 10 and -186°C. The strength of the specimen did not degrade and cracks were not observed in the specimen as a result of cyclic cooling.

Shahanian also reports that the 6061 aluminum material reinforced with silicon carbide coated boron sustained less strength reduction than the material that was reinforced with uncoated boron fibers. He attributed this effect to the reduced reactivity between the fiber and the matrix. There were no internal cracks observed.

F. THERMAL EXPANSION OF COMPOSITES

The standard equation for the mean coefficient of thermal expansion as used by Kreider and Patarini [39] is

$$\bar{\alpha} = \frac{\Delta L/L_o}{\Delta T} , \qquad (19)$$

where

$\bar{\alpha}$ = the mean thermal expansion coefficient,

ΔT = the temperature interval over which $\bar{\alpha}$ is being measured,

ΔL = the length change over the temperature interval, ΔT,

L_o = the initial sample length.

Turner [40] derived an equation for the prediction of the thermal expansion coefficient based on a condition of stress equilibrium. The equation is:

$$\alpha_c = \frac{\Sigma \alpha_n K_n V_n}{\Sigma K_n V_n} , \tag{20}$$

where

α_c = the thermal expansion coefficient of the composite,

α_n = the thermal expansion coefficient of the individual components,

K_n = the bulk modulus of the individual components

$$= \frac{E_n}{3(1-2\nu_n)} ,$$

V_n = the volume fraction of the individual components,

E_n = the elastic modulus of the individual components,

ν_n = the Poisson's ratio of the individual components.

For a two-component composite that consists of a homogenous matrix and fiber the equation becomes:

$$\alpha_c = \frac{\alpha_m E_m (1-V_f)(1-2\nu_f) + \alpha_f E_f V_f (1-2\nu_m)}{E_m (1-V_f)(1-2\nu_f) + E_f V (1-2\nu_m)} . \qquad (21)$$

Thomas [41] derived an equation for the composite thermal expansion coefficient which was based on a modification of the Rule of Mixtures. The equation is:

$$\alpha^c = V_f \alpha_f^c + V_m \alpha_m^c , \qquad (22)$$

where

α = the thermal expansion coefficient of the composite,

c = an empirically determined constant which can take any value between +1 and -1,

V_f , α_f , V_m , and α_m take on their usual values.

Both Turner's and Thomas' equations used elasticity theory to predict composite behavior. It has already been established that the aluminum matrix material

will undergo plastic deformation during temperature change. This is especially true for temperatures over 200°C because the yield point decreases dramatically above this temperature.

Kreider and Patarini [39] suggested a model that enabled the effect of matrix plasticity to be taken into account. They assumed that work hardening did not occur in the matrix. The equation that results from consideration of this model is given by:

$$\Delta T\ \alpha_c = \Delta T\ \alpha_f + \varepsilon_f\ , \tag{23}$$

where

$\Delta T\ \alpha_c$ = the axial expansion of the composite due to the temperature change,

$\Delta T\ \alpha_f$ = the expansion of the fiber due to the temperature change,

ε_f = the strain in the fiber due to internal stresses

$= \frac{\sigma_f}{E_f}$,

E_f = the modulus of the fiber.

Assuming there are no external forces on the composite, Equation (13) can be substituted into Equation (23) to give:

$$\Delta T\ \alpha_c = \Delta T\ \alpha_f - \frac{(1-V_f)\sigma_{my}}{V_f E_f} \quad , \tag{24}$$

where

σ_{my} = the yield stress of the matrix (negative when heating and positive when cooling).

Experimentally, Kreider and Patarini [39] showed that their plastic analysis could be used to predict the thermal expansion of composites. The specimens used were 2024 aluminum and 1100 aluminum reinforced with Borsic fibers.

G. CREEP OF COMPOSITES

Time-dependent deformation of material subject to applied stresses at elevated temperatures is called creep. Types of creep include primary, secondary, and tertiary. Primary creep is characterized by a decreasing rate of deformation under constant stress. Eventually the deformation rate will become constant. This constant rate creep is termed secondary creep. Tertiary or final creep is reached when the rate of deformation increases prior to final fracture.

Secondary creep is described by an Arrhenious-type of equation in which the magnitude of the strain rate is significantly influenced by an activation energy. A useful approximation of the steady-state creep rate is [36]:

$$\dot{\varepsilon} = Ae^{-(H/KT)} , \qquad (25)$$

where

A = a constant at a constant stress,

H = activation energy for creep which is constant at a constant stress,

K = Boltzmann's constant,

T = temperature.

According to McClintock and Argon [36], the rate of steady-state creep is controlled by some diffusion-controlled processes such as migration of vacancies between grain boundaries, grain-boundary sliding, grain-boundary migration, elimination of dislocation loops around precipitates, climb of edge dislocations out of slip planes, and drag of jogs on screw dislocations. But in many materials it is found that the activation-energy for creep is approximately the same as that measured for self diffusion.

The accelerating phase in the final stage of the creep process is due to the decrease in the cross-sectional area of the specimen, and the growth of internal cracks and voids [36]. Under certain conditions, recrystallization and overaging also contribute.

The creep behavior of metals is affected by a number of variables. The main variables include both

temperature and applied stress. Finnie and Heller [42] showed that creep becomes very important in materials exposed to temperatures that exceed a value approximately half the absolute melting-point temperature. Changes in temperature and alternating stress produce even more creep than would be expected under constant load conditions [36].

Slip, subgrain formation, and grain-boundary relaxation are the principal deformation processes at elevated temperatures. There are three main grain-boundary processes which are observed in high-temperature creep. The first process is grain-boundary sliding which is a shear process that occurs within the grain boundary itself. The second process is grain-boundary migration, defined by Dieter [43] as a motion of the grain boundary in a direction perpendicular to its plane.

Stress relaxation occurs when the strain of a material is held constant at a high temperature and the stress is allowed to vary. In a constant strain test carried out at elevated temperatures, the total strain is the sum of the elastic and plastic strains. The occurrence of significant plastic flow due to creep will tend to decrease the elastic portion of the strain and the stress applied to the material will be reduced. A rough estimation of stress relaxation can be made from the strain rates observed during creep. Essentially, tests are carried out

at several different stress levels and the resulting strain rate is monitored.

It is reasonable to assume that the majority of the creep process takes place at temperatures above one-half of the absolute melting point. A process analagous to fatigue will occur at lower temperatures. An investigation into temperature cycling, as described by Ellison [35], showed that the severity of the observed metallurgical structural changes increased progressively with time at elevated temperatures. This process caused a weakening of the material's strength and accelerated creep.

Prewo [44] has reported that boron fibers exhibit anelastic creep, that is, recoverable creep. Erickson [45] has noted a similar creep behavior for Borsic fibers. He showed that for temperature up to 300°C, the axial creep can be treated as logarithmic creep with activation energies between three and seven Kilocalories per mole (Kcal/mole). He concluded that the creep at room temperature of an aluminum-Borsic composite was controlled by the creep of the fibers. Antony and Chang [5] suggested that the creep in boron-aluminum composites measured at temperatures from 121 to 316°C is governed by the boron fibers.

Toth [46] observed three stages of creep in boron-aluminum composites tested at 204 and 316°C. The stages were strain on loading, elastic strain of the filament

(called the quasi-first stage), and strain controlled by the creep of the filament.

Breinan and Kreider [47] reported that the mean stresses for a 1,000-hour rupture life at 300, 400, and 500°C for an aluminum-Borsic composite were 96, 82, and 72 ksi, respectively. Aluminum composites reinforced with boron fibers showed similar short-time rupture strengths, but the stress for the material reinforced with uncoated boron fibers decreased more rapidly. According to the authors, this was due to the degrading reactions that occurred between the uncoated boron and the aluminum. The maximum plastic elongation corresponded to the creep of the fibers.

Pinnel and Lawley [48] concluded that the room-temperature creep in a stainless steel-aluminum composite was controlled by the creep of the fibers.

Breinan and Kreider [47] studied the transverse creep and stress-rupture of 6061 aluminum-Borsic composites. Those properties of the composites at 300°C were similar to the wrought matrix alloy with a similar heat-treatment.

All of these creep tests were carried out using a constant load. In the unidirectional test, the loads were relatively high. This suggests that at low loads and moderate temperatures the boron and stainless steel are creep resistant. Prewo [44] reports that this conclusion can be applied to silicon carbide fibers also.

The creep activation energy for aluminum is 3.4 Kcal/mole at room temperature, but increases to 35.5 Kcal/mole at 800°K. Reed-Hill [50] reported that between 600 and 700°K the activation energy is about 28 Kcal/mole. Breinan and Kreider [49] reported that the creep rate of a 6061 aluminum alloy was of the order 10^{-4} inch/inch/hour at 300°C at a constant stress of 3 ksi. Therefore, at temperatures above 600°K significant creep relaxation would be expected to occur in the aluminum matrix.

Wright [51] suggested that grain rotation in the aluminum matrix took place when boron-aluminum composites were thermally cycled.

CHAPTER III

EXPERIMENTAL PROCEDURE

A. TEST MATERIAL

The test material made by the Amercom Corporation consisted of nine 12 x 12-inch panels of aluminum matrix reinforced by three different types of fibers. In the panel fabrication, aluminum foil was placed between layers of fibers, heated to approximately 500°C, pressed together at high pressure and then slowly cooled. This process is called hot-press diffusion bonding.

Two of the panels were reinforced with 45 volume percent stainless steel fibers. One panel was fabricated in 1972 and the other in 1973. There were two composite panels fabricated; the 1972 panel contained 34 volume percent silicon carbide. Of the five remaining panels, two were fabricated in 1972 or 1973, each contained 27 volume percent unidirectional boron reinforcement. Two additional panels were fabricated in 1972 and 1973; each of these panels was reinforced with 45 volume percent 0° to 90° crossplied boron fibers. One additional panel, manufactured in 1973, consisted of 45 volume percent ±45° crossplied boron fibers.

The thickness of the stainless steel reinforced panels was about 0.02 inch. The silicon carbide reinforced 1972 panel was about 0.04 inch thick, but the thickness of

the 1973 panel of the same material was approximately 0.02 inch. The unidirectional boron-aluminum panels were about 0.06 inch thick, but the crossplied boron reinforced panels were approximately 0.05 inch thick.

The panels were cut into 6 x 0.5 inch longitudinal or transverse specimens. Transverse specimens were cut only from the panel fabricated in 1972. All but the stainless steel fiber were cut using electric discharge machining (EDM). Mechanical shears were used to cut the stainless steel reinforced material.

B. MECHANICAL PROPERTY DETERMINATION

The test specimens were prepared for the modulus and ultimate tensile strength tests by affixing 1.5 x 0.5 x 0.04-inch aluminum tabs at each end with Lafayette's Eccobond adhesive. The modulus of most of the specimens was obtained by using an Instron extensometer attached to the specimen by spring-loaded clamps. On some of the specimens, two longitudinal and two transverse Balwin, Lima, Hamilton (BLH) strain gages were affixed to the surfaces of the specimen in order to obtain the respective modulus values and Poisson's ratios.

A standard floor model Instron Tensile Test Machine was used to apply the load to the specimen at a cross-head speed of 0.02 inch per minute. The applied loads and the strain output from the extensometer or strain gages

were recorded on the Instron's recording chart. To insure that the axis of the fibers was in line with the load axis of the Instron, a spirit level was used to align the specimen. This technique was accomplished by assuring with the use of a spirit level that the Instron was level, and then the specimen was placed in the Instron in vertical position and checked with the spirit level. Thus, if the specimen was vertical, then the fiber axis was in line with the load axis of the Instron.

C. THERMAL CYCLING FURNACES

For the thermal cycling, four specimens were placed in a fixed position while an electrically-driven resistance heated furnace moved vertically over them. Cold air was blown across the specimens when they were outside the furnace in order to increase the cooling rate and bring the temperature of the specimen down to room temperature within the time allowed. The temperature of the furnace was controlled to within ±10°C by a Barber Coleman on/off controller.

The specimen temperature was monitored by feeding the output of a chromel-alumel thermocouple into an Assembly Products 10 ohms External Resistance Thermocouple Indicator. The thermocouple was placed touching the center of one of the specimens. The specimens were positioned along the axis

of the furnaces insuring that the specimens were always at the same temperature.

The cycling process consisted of heating and cooling the specimens between 425°C and room temperature. The time required to complete a cycle was varied by substituting a different timing motor in the circuit of the furnace drive mechanism. The cycling times used were three, six, and twelve minutes per cycle. The number of cycles was usually 6,000, but a few of the transverse specimens were cycled for ten cycles to determine if there were age-hardening effects on the matrix.

When the first group of transverse specimens was thermally cycled, the aluminum matrix was unable to support the weight of the composite. These specimens bent severely. Therefore, the remaining transverse specimens were placed between two thin stainless steel sheets and the bending of the transverse specimens was eliminated.

D. DILATOMETER

The thermal expansion of the unidirectional boron-aluminum composite was measured repeatedly during each of the three different cycle experiments.

The apparatus in which the thermal expansion was measured consisted of a carbon holder, a carbon pushrod, a BLH Linear Variable Differential Transducer (LDVT), and a BLH SR-4 Strain Indication.

As shown in Figure 1 of the appendix,[2] the boron-aluminum composite was placed in the carbon holder which was then positioned in the center of the vertical plane of one of the thermal cycling furnaces. A platinum-platinum, 13%-rhodium thermocouple was positioned near the center of one of the edges of the specimen. Then the carbon pushrod was inserted into the carbon holder and then positioned under the LVDT. As the pushrod moved up, the displacement caused the armature in the LVDT to shift; thus, enabling the movement to be recorded.

The thermal cycling furnace applied 6,000 cycles using a heating and a cooling periodicity that lasted three, six, or twelve minutes per cycle. Cold air was blown over the carbon holder to increase the cooling rate and reduce the specimen temperature to room temperature within the required time period.

A measured thermal gradient of 200°C existed over the entire length of the specimen, but the temperature was constant over the 3-inch gage length in the middle of the specimen.

The LVDT movement was calibrated for the strain indicator by positioning a micrometer in such a way that its movement coincided exactly with the movement of the carbon pushrod. The calibration curve is shown in Figure 2. The

---

[2]All subsequent figures appear in the appendix.

compensating resistance gage on the strain indicator was set for a gage factor of two. This gage factor was found to produce the maximum linearity in the calibration curve. Calibration of the system was completed using standard 6061 aluminum specimens which were thermally cycled in the dilameter for each of the cyclic periods. Because of the temperature gradient over the specimens, the actual thermal expansion of the aluminum specimen could not be determined. Thus, only the relative thermal extension was obtained by subtracting the measured thermal extension of the composites from the thermal extension of the standard aluminum specimen cycled with a corresponding cyclic period. The specimen temperature was recorded during a cycle for each of the different cyclic periods. The specimen temperature for each cyclic time is shown in Figure 3.

Seven or eight times per test of 6,000 cycles, the expansion of each specimen was monitored for ten to twelve cycles. The monitoring times were chosen so that four supervision periods occurred in the first 1,000 cycles. This resulted from the assumption that the maximum amount of extension would be obtained during this initial portion of the cyclic life. The rest of the measurements were evenly distributed throughout the remaining cycles. The results of the ten to twelve cycles of each of the monitoring times were examined. The cycles that caused the average final reading to deviate from ±0.0002 mm from zero were

disregarded. This was done because of an assumption which was based on the current literature [46] for creep of boron-aluminum composites that permanent strain in the material is negligible for that period of time. The results reported per monitoring time are the average relative expansion of at least seven cycles.

E. DENSITY TESTS

Since the specific gravity is numerically equal to the density, the composite densities were determined by the Archimedes method. This was accomplished by weighing the material in air and then weighing it again submerged in methyl ethyl Ketone (MEK) which wet the material thoroughly. The measurements were carried out using a balance which could be read to an accuracy of ±0.001 gram.

The formula used to determine the density of the composite was:

$$\rho_c = \frac{A\rho_{MEK}}{A + H + F}, \tag{26}$$

where

A = weight of specimen in air (gm),

H = weight of holder in liquid (gm),

F = weight of holder and specimen in liquid (gm),

ρ_{MEK} = density of methyl ethyl Ketone
(0.802 gm/cm^{-3}).

F. ERRORS

The experimental errors in this investigation arose from five sources. They were:

1. The error in determining the failure strengths of the composites.
2. The error in determining the elastic modulus and Poisson's ratio of the composites.
3. The error in determining the density of the composites.
4. The error in the monitoring of the temperature in thermal cycling and annealing tests.
5. The error in determining the thermal extension during thermal cycling.

In determining the strength of a composite, the cross-sectional area needed to be determined. The relative error in the determination of a length was given by:

$$\left|\frac{\Delta(\text{length})}{\text{length}}\right| . \qquad (27)$$

The readability of the micrometer was ±0.0001 inch. The average thickness was 0.065 inch for boron-aluminum, 0.020 inch for stainless steel-aluminum, and 0.046 inch for silicon carbide-aluminum. Using Equation (26), the relative

error in thickness measurements was calculated to be about 0.15% for boron-aluminum, 0.5% for stainless steel-aluminum, and 0.22% for silicon carbide-aluminum. The average width was about 0.50 inch; therefore, the relative error in the width measurement using Equation (26) was about 0.02%. The relative error of the cross-sectional area is given by:

$$\left|\frac{\Delta(\text{area})}{\text{area}}\right| = \left|\frac{\Delta(\text{width})}{\text{width}}\right| + \left|\frac{\Delta(\text{thickness})}{\text{thickness}}\right| . \qquad (28)$$

Thus, the relative error of the measurement of the cross-sectional area calculated from Equation (27) was approximately 0.7% for boron-aluminum, 0.24% for silicon carbide-aluminum, and 0.52% for stainless steel-aluminum.

The final element in determining the failure strength of the composites is the applied load. The relative error in load measurements is given by:

$$\left|\frac{\Delta\ \text{load}}{\text{load}}\right| . \qquad (29)$$

The load readability was 1% full scale. The majority of the failure loads of the different composite materials occurred in the 5,000 pounds full scale load range. The smallest load that was measured in this load range was 2,083 pounds. Thus, the maximum relative error of the load determination using Equation (29) is about 2.4% for all the material.

The relative error for the failure stress determination is given by:

$$\left|\frac{\Delta \text{ stress}}{\text{stress}}\right| = \left|\frac{\Delta \text{ area}}{\text{area}}\right| + \left|\frac{\Delta \text{ load}}{\text{load}}\right| . \qquad (30)$$

The maximum relative error for the stress determination is 2.62% for boron-aluminum, 2.64% for silicon carbide-aluminum, and 2.92% for stainless steel-aluminum.

The errors associated with the determination of the elastic modulus and Poisson's ratio are caused by the electronics of the system, the load determination, and the strain determination.

The electronic error of the extensometer system is 0.25% according to the manufacturer. The electronic error of the strain gages that were bonded to the specimens was 0.2% as determined by the producer. The maximum relative error obtained from the load determination using Equation (28) was 1.25% for the 200-pound full scale load range.

The relative error in strain measurement is given by:

$$\left|\frac{\Delta \text{ strain}}{\text{strain}}\right| . \qquad (31)$$

The extensometer and the strain gages that were affixed to the surface of specimens had a readability of ±0.0001. The largest strain measured for the material was 0.006 which

would give the maximum error. The maximum relative error in the determination of strain was about 1.67%.

The relative error in the determination of the elastic modulus is given by the equation:

$$\left|\frac{\Delta \text{ modulus}}{\text{modulus}}\right| = \text{electronic errors} + \left|\frac{\Delta \text{ load}}{\text{load}}\right| + \left|\frac{\Delta \text{ strain}}{\text{strain}}\right| . \quad (32)$$

The maximum relative error is calculated using Equation (32) to be approximately 3.17% for the extensometers and 3.12% for the strain gages.

The relative error of the determination of Poisson's ratio is given by the equation:

$$\left|\frac{\Delta \text{ Poisson's ratio}}{\text{Poisson's ratio}}\right| = \left|\frac{\Delta \text{ modulus}}{\text{modulus}}\right| + \left|\frac{\Delta \text{ strain}}{\text{strain}}\right| . \quad (33)$$

The maximum lateral strain is measured to be about 0.002 inch/inch. Using Equation (33) the maximum relative error in determining Poisson's ratio was 5.0%.

The error in determining the density is totally dependent on the error in weight measurement. The relative error is given by:

$$\left|\frac{\Delta \text{ density}}{\text{density}}\right| = \left|\frac{\Delta \text{ weight}}{\text{weight}}\right| . \quad (34)$$

The readability of the chemical balance was ±0.001 gram. The maximum average weight was about 2 grams. Therefore, using Equation (34), the maximum relative error of determining the density is 0.05%.

The error in temperature measured was due to the electronic error of the readout meter. The accuracy of that device was 1% of full scale as determined by the producers. This made the readability of the K-type thermocouple ±11°C, and the R-type thermocouple ±1°C. The relative error of the temperature determination is given by:

$$\left|\frac{\Delta \text{ temperature}}{\text{temperature}}\right| . \qquad (35)$$

The temperatures that were of interest were 20°C and 425°C. The relative error at the low temperature was approximately 55% with the K-type thermocouple, and 5% with the R-type thermocouple. The relative error at the high temperature was about 2.6% with the K-type thermocouple, and 0.23% with the R-type thermocouple determined by Equation (35).

The error associated with measuring the thermal expansion of the composites was dependent on the electronic error of the strain indicator and the LVDT. The strain indicator had an accuracy of ±0.0037 mm. The LVDT had an accuracy of ±0.005 mm full scale. The average maximum extension measured was about 0.033 mm. The relative error of the determination of the extension is given by:

$$\left|\frac{\Delta \text{ extension}}{\text{extension}}\right| . \qquad (36)$$

The readability of the entire system is ±0.0087 mm. Therefore, the relative error of the system is about 26.4% as calculated by using Equation (36).

CHAPTER IV

RESULTS

A. ULTIMATE TENSILE STRENGTHS

1. Stainless Steel-Aluminum Composites

The unidirectional strengths of the specimens reinforced with stainless steel fibers in the as-received condition are compared to thermally cycled specimens in Table I of the appendix.[3] As can be observed, there was a difference of approximately 20% in the unidirectional strength of specimens cut from the 1972 as-received panel as compared to those that had been thermally cycled using the three-minute period. Specimens cut from the 1973 panel exhibited a reduction in strength of about 11% when the as-received specimens are compared to those that had been cycled using the six- and twelve-minute period.

The maximum cyclic temperature had to be lowered to 365°C cyclic temperature; the fibers had bowed away from each other and the matrix had disintegrated. However, with the transverse specimens, 425°C was used as the maximum cyclic temperature with no sign of matrix disintegration. The fiber separation that occurred in the unidirectional material was expected if it were assumed that the matrix

[3]All subsequent tables appear in the appendix.

constrained the stainless steel fibers at room temperature. During the thermal cycling process the matrix would relax at high temperature and the fibers would separate. This fiber separation did not occur in a specimen that was statically loaded. Thus, the assumption of matrix constraint on the stainless steel at room temperature appeared to be valid. In the transverse material, the constrained stresses on the short fibers were not great enough to allow the fibers to bow away from each other.

The transverse strength of the stainless steel reinforced material suffered a 33% decrease when cycled using a three-minute period.

2. Silicon Carbide-Aluminum Composites

The strength of the as-received unidirectional silicon carbide reinforced material fabricated in 1972 or 1973 was identical, as shown in Table II. Specimens exhibited a small drop in strength when cycled at the three-minute period. However, the magnitude of the reduction increased to 30% for specimens subjected to the six- and twelve-minute cyclic periods.

The transverse strength was obtained after ten cycles using a three-minute cyclic period and the results were compared to the as-received material. There was little change. However, after 6,000 thermal cycles were performed using the same period, there was a 45% strength loss.

3. Boron-Aluminum Composites

As shown in Table III, the tensile strength of all the boron-aluminum composites decreased with thermal cycling. The 27 volume percent unidirectional material decreased 39% using the three-minute cyclic process, 61% using the six-minute process, and 80% using the twelve-minute process. The strengths of the 1972 and 1973 panels were about the same for this material. The strengths of the 45 volume percent 0° to 90° crossplied material were approximately equal for specimens cut from the 1972 panel and 1973 panel, and these results are reported in Table IV. Specimens cut from the crossplied material exhibited a strength loss of 35% after thermal cycling using the three-minute process, 70% using the six-minute process, and 90% using the twelve-minute process. In the 45 volume percent ±45° crossplied material, the decrease in composite strength, reported in Table V, was 31% for the three-minute cyclic period and 70% for the six- and twelve-minute periods.

A specimen cut from the 1973 panel was fully annealed. The procedure followed was the standard procedure for annealing 6061 material [51]. The specimen was kept at 775°F for 2.5 hours and then air cooled. The strength of the material in the as-received condition was about 128 ksi as compared to 121 ksi for the material in fully annealed condition. Thus, the as-received material was close to being fully annealed.

The transverse specimens containing 27% boron fibers showed a strength loss of about 50% for the three-minute and the six-minute cyclic periods as compared to the as-received conditions.

B. ELASTIC MODULUS, DENSITY, AND POISSON'S RATIO

As reported in Table I, the elastic modulus dropped slightly during thermal cycling, but the length of the cyclic period had little effect on the properties of the stainless steel composites. The same statement also describes the densities measurements except for the specimens in which the matrix had disintegrated.

As shown in Table II, the modulus of the unidirectional silicon-carbide reinforced composites decreased slightly for specimens subjected to the three-minute cyclic period, but a further decrease of about 37% was exhibited by these specimens subjected to the six- and twelve-minute periods. The density for the unidirectional material decreased as the cyclic period increased. A 29% drop in the modulus was observed in the transverse reinforced material when cycled at a three-minute period.

Thermal cycling caused a decrease in the modulus values for all of the boron-aluminum composites. The results, noted in Tables III, IV, and V, demonstrated that the decrease was small in the 27 volume percent unidirectional material for all the cyclic periods except

the twelve-minute period. In this case there was a 32% decrease. The modulus of the transverse reinforced material showed a slight reduction after thermal cycling using a three-minute period, and a 19% decrease using a six-minute period. The 0° to 90° crossplied material's modulus declined 22% using a three-minute period, and 37% using the six- and twelve-minute periods. The modulus of the ±45° crossplied material dwindled with increasing cyclic period.

The densities of the off-axis boron reinforced material decreased with increasing cyclic period. However, the densities measured for the 0° to 90° reinforced specimens that were subjected to the six- and twelve-minute cyclic periods were approximately equal.

The values of the major Poisson's ratio for the unidirectional reinforced material were reported to be about 0.25. This Poisson's ratio value agreed rather well with the value reported by Allred, Hoover, and Horak [52]. These authors have shown that the Rule of Mixtures could be used to predict Poisson's ratio for a composite.

C. THERMAL EXPANSION DURING CYCLING

In order to make the results of the thermal expansion experiment relative, the measured thermal extension of the boron-aluminum specimen was subtracted from the thermal extension of standard 6061 aluminum samples that was measured in the same manner as its corresponding

composite specimen, that is, the thermal extension of the composite specimen cycled with a three-minute period was subtracted from the thermal extension of the aluminum specimen cycled with a three-minute period, and so forth. The results were calculated as a function of the specimen temperature during an average cycle and are reported in Tables VI, VII, and VIII. The thermal extension of the composite specimens was monitored at various cycles during the total thermal cyclic life. Since the thermal expansion of the aluminum samples was greater than that of the composite specimens, the greater amount of difference between the thermal extension of the aluminum and that of the boron-aluminum meant that the relative thermal expansion of the composites was smaller.

In general, the relative thermal expansion of the composite cycled with a three-minute period was more than that of the specimen cycled with a six-minute period. The six-minute specimen expanded more than the twelve-minute specimen. In all cases, there was a lag in the relative thermal contraction of the composites at the beginning of the cooling portion of the average cycle.

The relative thermal extension of the boron-aluminum material cycled using a three-minute period generally expanded more at the start of its cyclic life than it did at the finish. The average cyclic extension of this specimen decreased rapidly for the first 500 cycles. Then

there was an increase in the average thermal extension. Finally, the thermal extension reached a fairly constant value with the last 1,000 cycles.

Concerning the relative thermal extension of the six-minute period composite specimen, there was a general increase in average extension from the first cycles to that of the last cycles during the heating portion of the cyclic life. However, during the cooling portion, the average extension decreased from the first to the last cycles. The average thermal extension for this material decreased for the first 1,000 cycles for both the heating and cooling portions of the cyclic life. Then the average expansion increased for the remaining cycles.

The relative thermal extension of the twelve-minute period specimen expanded more at the beginning of the thermal cycles than at the end. There was a decreasing average thermal expansion for this specimen during the first 100 cycles followed by an increase in extension during the next 300 cycles. During the last 1,000 cycles the average extension attained a fairly constant value.

During the total life of all the cyclic periods, there was an overall contraction from the initial length. The overall contraction decreased as the cyclic period increased.

D. METALLOGRAPHIC AND GENERAL OBSERVATIONS

Figures 4 and 5 show the results of the unidirectional boron-aluminum material subjected to thermal cycling with a three- and twelve-minute cyclic period, respectively. These observations were made after the specimens had been cycled for 6,000 cycles. The intensity of the surface damage increased with an increasing cyclic period. The surfaces, for the most part, consisted of a series of ridges which were perpendicular to the fiber direction. Closer observations using a Scanning Electron Microscope, showed that at the base of a twelve-minute cyclic period specimen there were surface cracks that extended into the specimen.

The surface of a 0° to 90° crossplied material after 6,000 cycles becomes extensively disrupted with a progressively increasing period. The damage is in the form of square-based spheroids as viewed with a Scanning Electron Microscope shown in Figure 6. The fiber geometry can be identified from surfaces of the unidirectional and crossplied material.

Observations made with a Scanning Electron Microscope of the 0° to 90° boron reinforced material that was thermally cycled using the twelve-minute period, appearing in Figure 7, indicated an apparent grain boundary process. Each of the square-based spheroid's cells had an average diameter of between 10^{-3} to 10^{-4} inches [51].

The surfaces of the silicon carbide reinforced material have round spheroids as the surface damage. The damage becomes more intense as the cyclic period increased. These results are pictured in Figures 8, 9, and 10.

As can be seen in Figures 11, 12, and 13, the surfaces of the stainless steel-aluminum material show surface damage that is approximately the same for each of the cyclic periods. These observations are made from specimens where 365°C is used as the maximum cyclic temperature.

The photograph, shown in Figure 14, displays the surface of a boron-aluminum specimen after being progressively thermally cycled using a six-minute period with a maximum cyclic temperature of 425°C. The results show a network of grain boundaries after a very few cycles. The surface becomes extremely rough after about 50 cycles, making it difficult to focus on the individual surface grains which indicates that the grains are moving. The average grain diameter is between 10^{-3} and 10^{-4} inches.

The silicon carbide reinforced material's cross-sectional area expanded after thermal cycling. There was a 10% average expansion in width and a 19% average expansion in thickness for the three-minute period specimen. Expansion was about the same for the specimens subjected to

the six- and twelve-minute cyclic periods. The average expansion was about 19% for the width and 33% for the thickness.

CHAPTER V

DISCUSSION

A. THEORETICAL ULTIMATE TENSILE STRENGTHS OF UNIDIRECTIONAL COMPOSITES

1. Brittle Fibers

As discussed in Chapter II, there is no unique value for the strengths of brittle fibers. The theoretical tensile strength of silicon carbide reinforced composites and boron reincorced composites must therefore be expressed as a range of values. The range of composite strength values based on a statistical distribution of fiber strength is bounded by an upper and lower limit. Rosen [29] has reported that the lower bound strength is derived by assuming the fiber-matrix bond is weak and by assuming the composite has the strength characteristics of a bundle of fibers. The strength of a bundle, σ_B , is given by Equation (7). Thus, assuming that the matrix carries no shear loads, the lower bound strength, σ_{cL} , of a composite is determined by:

$$\sigma_{cL} = V_f \sigma_B \ , \tag{8}$$

where

V_f = the volume fraction of fibers.

The gage length of the specimen is utilized in the determination of the bundle strength of the fibers.

The upper bound strength of the composite material can be calculated by using the cumulative damage theory discussed by Rosen [28]. A strong fiber-matrix bond is assumed when using this theory. As discussed by the author, the composite system can be considered as a number of layers, each with a length equal to the ineffective length connected in series. The section of fiber within a layer may be considered as a link in a chain which constitutes the entire fiber. Each layer can be considered as a bundle of these links, and the composite is a series of bundles. Failure of the composite occurs when one of these bundles fails.

Values for the strength of a bundle of fibers having an ineffective length, δ, can be calculated from the equation:

$$\sigma_B = \sigma_o \left(\frac{\delta}{d}\ \omega e\right)^{-1/\omega} . \tag{9}$$

The ineffective length, according to Rosen [22], is computed by using the equation:

$$\delta = \frac{\sigma_d}{2\tau} . \tag{11}$$

In this model, σ is assumed to equal the value of σ_B given in Equation (9). Equation (11) is then substituted into

Equation (9) and the upper bound of composite strength, σ_{cu}, is determined by using the equation:

$$\sigma_{cu} = V_f \sigma_o \left(\frac{\delta}{d}\ \omega e\right)^{-1/\omega} + (1-V_f)\sigma_m \ . \qquad (10)$$

Unfortunately, the values, σ_B and δ, are found to be interdependent. Thus, the ineffective length and upper bound strength are determined by computing these values iteratively until both equations (Equations (9) and (11)) are satisfied.

For this work the values used to determine the upper and lower bounds of the composite strengths were obtained from data reported by Wright [51]. The results are tabulated in Table IX, along with the experimental strength values of the specimens from which the fibers were extracted.

The as-received strength of the silicon carbide reinforced material is approximately equal to the theoretical lower bound calculated from the extracted fibers. There was no apparent loss of strength for these fibers extracted from the thermally cycled specimens. However, the strength of the thermally fatigued specimens was degraded. The strength of the boron reinforced material subjected to thermal cycling using the twelve-minute period was well below the theoretical lower bound composite strength.

A decrease in strength of the thermally cycled boron-aluminum specimen was observed. The theoretical lower

bound strength of the composite was calculated by utilizing the strength data obtained from fibers extracted from a specimen that had been thermally cycled using a twelve-minute period. The result indicated that the strength was 80% more than the strength of the composite obtained experimentally.

A simple experiment was carried out on the boron and silicon carbide reinforced material. The fibers present in the as-received and the twelve-minute thermally cycled boron or silicon carbide reinforced material were counted by examining a cross-section of each specimen using a low-powered microscope. Some of the specimens had been subjected to tensile tests so only half of the total length was used for this experiment. The fibers from the composite material were then extracted and counted. The results of this experiment are given in Table X. The excess fibers are broken portions of originally continuous fibers. For the composites subjected to tensile tests, the number of fibers that were counted were multiplied by two to account for the other half of the broken specimen.

According to Wright and Wills [10], if there is a small number of multiple fiber breaks present in a composite material, the bundle failure mode is suggested. It has been substantiated in a previous section that the strengths of the boron and silicon carbide specimens cycled using a twelve-minute period were well below the strengths predicted

using bundle theory. Thus, as the strength of the composite material decreases due to thermal cycling, the number of breaks should decrease.

The number of fiber breaks contained in the specimen thermally cycled using a twelve-minute period was greater than the same material in the as-received condition. Since a fiber could break more than once, the number of broken fibers at failure of the specimen cannot be estimated exactly; however, it can be concluded that the thermally cycled material contained more broken fibers than the as-received material. Thus, the thermal cycling process using a twelve-minute period caused many of the fibers to break.

This conclusion also explains the observation that the experimental composite strengths are less than the theoretical lower bound. The calculation of the lower bound strength from extracted fibers assumes that all the fibers in the composite contribute to the load bearing capacity of the material. Broken fibers cannot carry any load if the material behaves as a simple bundle. Thus, the actual strength values would tend to be lower than the theoretical lower bound strength of the composite.

2. Ductile Fibers

The theoretical strengths of composites reinforced with stainless steel fibers, reported in Table X, were calculated using the Rule of Mixture:

$$\sigma_c = V_f\sigma_f + (1-V_f)\sigma_m \ . \qquad (4)$$

The values of σ_f were obtained from extracted fiber data reported by Wright [51], and σ_m was measured to be 29 ksi by White [53]. The mean strength value of the material was 239 ksi for a specimen cut from the panel fabricated in 1972, and 148 ksi for a specimen cut from the panel fabricated in 1973. The experimental and theoretical strengths of this material thermally cycled using a three-minute period were 193 ksi and 239 ksi, respectively.

The decrease in strength of the thermally cycled material from its as-received strength can be discussed in terms of the degradation of the interfacial bond.

B. DEGRADATION OF THE FIBER-MATRIX BOND

Metcalfe [4] has concluded that the strength of an aluminum matrix composite degrades by a mechanism that involves the disruption of a bond that exists between the oxide film of the fiber and the matrix material. The breakdown of the bond is caused by mechanical shear. This shear force is generated, for example, by plastic deformation that

often occurs when the composite is subjected to large temperature variations. In the case of a boron-aluminum composite, Metcalfe [4] has reported that the breakdown of the fiber-matrix oxide film results from the chemical reaction of the aluminum with the boron fiber. This interfacial bond is degraded severely when an excessive reaction occurs between the boron and aluminum. The strength of the boron fiber is also reduced.

It has been reported [6, 8, 9, 37] that the strength of boron-aluminum fiber composites decreased if the specimen was subjected to high temperatures for extensive time periods. Also, Wright [37] deduced that a part of the composite strength reduction in thermally fatigued boron-aluminum was the result of the degradation of the interfacial bond.

The strengths of all the 27 volume percent boron-aluminum material tested in this investigation decreased when the specimens were thermally cycled. Wright and Wills [10] reported that part of the strength degradation of similar thermally fatigued material resulted from degradation in the strength of the fibers. However, the magnitude of the decrease of the composite's strength was larger than could be explained solely by this fiber strength degradation. As reported in Table XI, the strength values of the composites suffered an additional decrease that effectively reduced the strength towards the lower strength

bounds. This effect was more pronounced for those specimens subjected to the longer period of cyclic temperature change.

The additional decrease in the composite strength over and above that which can be explained by the degradation of the fiber strength has been attributed to the degradation of the fiber-matrix bond. The reduction in the transverse strength of the boron-aluminum material also suggests that the strength of the fiber-matrix bond is degraded by the thermal fatigue process.

It can be inferred from the work of Chen and Lin [18] that the transverse strength with no interfacial bonds would be lower than that exhibited by a well bonded composite. It was also noted from their report that the transverse composite strength will not be expected to exceed the tensile strength of the matrix. Cooper and Kelly [20] have shown that the theoretical transverse strength of a composite can be described by the equation:

$$\sigma_t = \sigma_m\left(1 - \sqrt{\frac{4V_f}{\pi}}\right) + \sigma_i'\left(\sqrt{\frac{4V_f}{\pi}}\right), \qquad (3)$$

where σ_i' is the stress required to break the fiber-matrix bond.

Inspection of the above expression leads to a conclusion identical to that noted above, that is, the transverse strength of a composite will never be greater than the tensile strength of the matrix. If the fiber-matrix

bond strength, σ_i' , is zero, then the transverse strength will decrease progressively as more fibers are added to the matrix. Conversely, if the strength of the fiber-matrix bond is effectively infinite, then the composite would behave as if it were fabricated from matrix alone. The transverse strength of the composite would then be identical to the tensile strength of the matrix.

Some indication of the relative strength of the bond between the fibers and the matrix for all the materials investigated in this study can be obtained by substituting typical values into Equation (3). The results of experiments performed at The University of Tennessee Space Institute [53] indicate that the as-quenched strength of 6061 aluminum is about 29 ksi. This value was obtained from a transverse test carried out on the specimens containing 27 volume percent boron fibers. However, it might be expected by equating both σ_m and σ_i' to 29 ksi in Equation (3).

By rearranging Equation (3), the average tensile strength necessary to separate the fiber from the matrix under transverse loading is found by the equation:

$$\sigma_i' = [\sigma_t - \sigma_m(1 - \sqrt{\frac{4V_f}{\pi}})] \; / \; \sqrt{\frac{4V_f}{\pi}} \; . \qquad (39)$$

Wright [54] reported that the strength of the 44% boron reinforced material used in his work was 21 ksi. Thus,

the tensile strength of the matrix of his material was probably slightly higher than that used in this investigation. However, inspection of Equation (39) indicates that a relative value of the fiber-matrix bond for the 44 volume percent material would be about 18 ksi. This is less than the value of 29 ksi computed from the results obtained in this work.

Using Equation (39), σ_i' was calculated to be 12 ksi and 14 ksi for the silicon carbide and stainless steel reinforced material, respectively. Thus, the relative interfacial bond strength decreased progressively, from the stronger boron-aluminum composite to the stainless steel reinforced material to the weaker silicon carbide reinforced material.

The effect of thermal cycling on the strength of the interfacial bond can also be studied by substituting the respective transverse strength values into Equation (39). Unfortunately, values have only been obtained for the specimens reinforced with silicon carbide and stainless steel fibers subjected to the three-minute cyclic period. The values of σ_i' were computed to be about 3 ksi and 6 ksi for the silicon carbide and stainless steel reinforced materials, respectively. The materials transversely reinforced with boron fibers were subjected to elevated temperatures using three- and six-minute cyclic periods. The value of σ_i' for this material was about 7 ksi for those

specimens subjected to the three-minute period and 4 ksi for those subjected to the six-minute period. These values are appreciably below those computed for the as-received specimens. This data supports the tentative conclusion [37, 51] that the fiber-matrix bond strength is degraded by the thermal cycling process.

C. EFFECT OF THERMAL CYCLING ON ELASTIC MODULUS

Intuitively, it is expected that the strength of the composite approaches the strength of a simple bundle of fibers as the strength of the fiber-matrix bond approaches zero. However, any broken fiber present in the composite will not contribute to the load-bearing capacity of the bundle. Thus, in addition to a strength decrease, the effective stiffness of the bundle will also be decreased. As determined previously, there are more fibers extracted from the silicon carbide and boron reinforced material subjected to thermal cycling using a twelve-minute period than were counted in a polished cross-section. It is concluded that many were broken by the cyclic treatment. In addition, the actual strengths of these composites were lower than the theoretical lower bound strength. The decrease in actual strength below that of the theoretical lower bound strength is about 45% for the boron-aluminum material with a corresponding decrease in stiffness of about 30%. The number of broken fibers in the boron-aluminum

material was estimated to be well over one-half the original number of fibers. And, since the composite behaved as a simple bundle and no load was being transferred between the fibers, the reported decrease in modulus of the twelve-minute, thermally cycled material is not expected. The number of broken fibers in the silicon carbide-aluminum material was about one-half of the original number of fibers. The decrease in actual strength below that of the theoretical lower bound strength was about 21% with a corresponding decrease of about 34% in the stiffness. The similarity between the magnitude of the decrease in the strength and modulus indicates that the reductions probably result from the same mechanism. However, a more quantitative correlation involving the total number of broken fibers is difficult because a fiber can possibly break more than once. This means that a number of broken fibers calculated from counting extracted fibers will be greater than the actual number.

D. CRACKS AND VOIDS IN THE MATRIX

Shahanian [38] reported that the thermal cycling of composite materials reinforced with silicon carbide coated boron fibers produced an expansion of the cross-sectional area of the specimens. He attributed this expansion to the growth of voids within the matrix. Kreider, Dardi, and Prewo [7] reported an expansion in width

of thermally fatigued Borsic-aluminum composites. In addition to this expansion, a reduction in the density of the specimens was observed. It was concluded that this effect resulted from the formation of voids or cracks in the matrix.

In this investigation, it was noted that there was an increase in the average cross-sectional area of the thermally cycled silicon carbide-aluminum material. The average increase was found to be 0.0062 square inches for material cycled with a three-minute time period, 0.0063 square inches for material cycled with a six-minute time period, and 0.0066 square inches for material cycled with a twelve-minute time period. In addition, a decrease in the average density was observed. As determined from Table II, the decrease in density was 0.193, 0.109, and 0.281 gram per cubic centimeter for specimens subjected to three-, six-, and twelve-minute cyclic periods, respectively. Thus, this silicon carbide reinforced material exhibited many of the same characteristics displayed by the thermally cycled composites reinforced with silicon carbide coated boron fibers. In agreement with the work of Kreider, et al., discussed above, it was concluded that the thermal cycling of silicon carbide-aluminum composites resulted in the growth of voids and cracks within the matrix. As shown in Figure 15, the thermal cycling of boron-aluminum composites also resulted in void formation near the fiber-matrix interface.

E. THERMAL EXPANSION OF COMPOSITES DURING THERMAL CYCLING

The thermal expansion of a unidirectional boron-aluminum composite can be discussed in terms of the thermal expansion coefficients of each of the components, for both components contribute to the total expansion of the system. The aluminum tends to expand more than the boron, but it will be constrained by the fiber-matrix bond. If there is no bond, the aluminum will expand freely. Thus, in this case, the expansion of the composite will be identical to the expansion of the matrix. The minimum amount of thermal expansion of the composite will be governed by the constraining effect of the boron fiber.

Unfortunately, the actual thermal expansion of the specimens used in this work could not be measured because of the thermal gradient along the length of the specimens. However, the results of this experiment were taken to indicate the type of processes taking place during thermal cycling. Thus, the thermal expansion of one of the boron-aluminum samples could be compared to the other samples of this same material treated identically using a different time period. It was reasoned, that as the bonding between the fiber and matrix deteriorated the magnitude of the thermal expansion would change.

The results of the thermal expansion experiment are plotted in Figures 16, 17, 18, 19, 20, 21, and 22.

Several changes in the relative expansion occur as the cyclic period varied. Also, variations are observed in expansion as the accumulated number of cycles of a specimen increased.

First, the relative maximum expansions of the specimen subjected to the three-minute cyclic period were greater than the expansions of the specimen subjected to the six-minute period. Furthermore, the thermal expansions of the six-minute specimen were greater than that of the specimen thermally cycled using the twelve-minute period. Using Equation (24), it was noted that the only variable that would effect the thermal expansion of a composite ($\Delta T\ \alpha_c$) is the matrix yield strength, σ_{my}. The results indicate that the expansion was related to the temperature dependence of the yield stress. The longer the specimens remained at the high temperature, the thermal expansion of the specimens more closely approximated that of the boron fibers.

Intuitively, it is reasoned that as the boron-aluminum composite is heated, the stress placed on the fiber by the difference in the thermal expansion coefficients of the fiber and matrix is an important force that determines the thermal expansion of the composites. As the temperature of the specimen increases above 200°C, local yielding begins to occur in the matrix. Also, as discussed in Chapter II, significant creep relaxation of the aluminum matrix is

expected to occur at temperatures over 600°K [32]. Thus, as the time at temperatures over 600°K increases, the stress on the fiber that is due to the thermal expansion of the matrix decreases, allowing the fiber expansion to become the dominant part of the total expansion of the composite.

As can be seen from Figures 16 through 22, during the cooling of each specimen, the contraction of the composite specimen was identical to that of a similar specimen cut from a 6061 aluminum panel until a temperature of approximately 125°C was reached. Since the difference in the thermal contraction coefficients that existed between the aluminum standard specimens and the composite was not changed, it was reasoned that this lag resulted from the very rapid change in temperature that initially occurred in the measurement device on cooling.

The relative thermal expansions of the various specimens are plotted for the different cycles at specified temperatures in Figures 23, 24, and 25. For the most part, these expansions are constant over the various cycles.

It has already been concluded that the deterioration of the bonding between the fiber and matrix increased as the cyclic period increased. As previously hypothesized, when the bonding breaks down, the aluminum will expand freely. However, there is always, at least, a friction bond between fiber and matrix. Therefore, as the bonding

decreased, the expansion of the composite should increase somewhat. This conclusion is supported by the expansions after the first 2,000 cycles increase as the cyclic period increased.

CHAPTER VI

CONCLUSIONS

1. The aluminum matrix of the fiber reinforced material investigated sustained significant damage when thermally cycled to a maximum temperature of 425°C.
2. The damage inflicted on the matrix due to thermal cycling increased as the thermal cyclic period increased.
3. There was a strength degradation in the composite material when thermally cycled.
4. The boron-aluminum strengths decreased as the cyclic period increased.
5. The aluminum matrix material reinforced with silicon carbide and stainless steel fiber showed a decrease in strength with an increase in cyclic period except for the six- and twelve-minute periods, which were similar.
6. The thermal cycling of the unidirectional stainless steel-aluminum material with a maximum cyclic temperature of 425°C resulted in severe damage to the matrix and degradation of its properties.

7. The thermal expansion, during the cyclic process, decreased with the increase of the cyclic period in the boron-aluminum material.
8. During the first few cycles of the thermal cycling process, grain boundary migration was observed in the boron-aluminum material.
9. Thermal cycling of the silicon carbide and boron reinforced material resulted in the breakage of fibers.
10. Thermal cycling of the aluminum matrix composite material resulted in the reduction of the elastic modulus.

CHAPTER VII

RECOMMENDATIONS

1. More observations are needed of the fiber-matrix interface in order to investigate the reaction between the fibers and matrix of the different materials. The best results might be obtained from an observation of the fracture surface of the different cyclic periods on the material reinforced with boron and silicon carbide. Quantitative observations could be made with a Scanning Electron Microscope.
2. In this investigation, the composite specimens were cut from respective panel and then thermally cycled. In order to reduce chance of property variation in the different samples due to changes in the cycling conditions, it would be more efficient to cycle a complete panel and then cut the specimens.

BIBLIOGRAPHY

BIBLIOGRAPHY

1. Metcalfe, A. G. "Introduction and Review," Composite Materials - Volume 1, Interfaces in Metal Matrix Composites. A. G. Metcalfe, editor. New York: Academic Press, Inc., 1974. Pp. 1-30.

2. Klein, M. J., and A. G. Metcalfe. "Effect of the Interfaces in Metal Matrix Composites on Mechanical Properties," Air Force Materials Laboratory TR-71-189, Wright-Patterson Air Force Base, Ohio, October, 1971.

3. Ebert, L. J., and P. K. Wright. "Mechanical Aspects of the Interface," Composite Materials - Volume 1, Interfaces in Metal Matrix Composites. A. G. Metcalfe, editor. New York: Academic Press, Inc., 1974. Pp. 31-64.

4. Metcalfe, A. G. "Physical Chemical Aspects of the Interface," Composite Materials - Volume 1, Interfaces in Metal Matrix Composites. A. G. Metcalfe, editor. New York: Academic Press, Inc., 1974. Pp. 31-64.

5. Antony, K. C., and W. H. Chang. "Mechanical Properties of Al-B Composites," Transactions of the American Society of Metals, 61:550-558, September, 1968.

6. Stuhrke, W. F. "Solid-State Compatibility of Boron Aluminum Composite Material," Metal-Matrix Composites. Columbus, Ohio: Defense Metals Information Center, Battelle Memorial Institute, 1969. Pp. 43-45.

7. Kreider, K. G., L. Dardi, and K. Prewo. "Metal Matrix Composite Technology," Air Force Materials Laboratory TR-71-204, Wright-Patterson Air Force Base, Ohio, December, 1971.

8. Klein, M. J., and A. G. Metcalfe. "Effect of the Interfaces in Metal Matrix Composites on Mechanical Properties," Air Force Materials Laboratory TR-72-226, Wright-Patterson Air Force Base, Ohio, November, 1972.

9. Wright, M. A., and B. Intwala. "The Effect of Elevated Temperatures on the Mechanical Properties of B-Al Composites," Journal of Material Science, Part VIII, 7:957-963, July, 1973.

10. Wright, M. A., and J. L. Wills. "The Tensile Failure Mode of Metal Matrix Composite Materials," Journal of Mechanics and Physics of Solids, 22:1-15, 1974.

11. Pattnaik, A., and A. Lawley. "Mechanical Behavior of Aluminum-Stainless Steel Composites Subjected to Elevated Temperature Exposure." Technical Report No. 6 prepared under Navy Contract No. N00014-67-A-0406-0001 by Drexel University, Philadelphia, Pennsylvania, March, 1971.

12. Baker, A. A. "The Effect of Fibre Volume Fraction and Interfacial Bond on the Fatigue of Aluminum Reinforced with Stainless Steel Wires," Applied Materials Research, 5:143-153, July, 1966.

13. Pinnel, M. R., and A. Lawley. "Correlation of Uniaxial Yielding and Substructure in Aluminum-Stainless Steel Composites," Metallurgical Transactions, 1:1337-1348, May, 1970.

14. Jones, R. C. "Deformation of Wire Reinforced Metal Matrix Composites," Metal Matrix Composites. ASTM Special Technical Publication No. 438. Philadelphia: American Society for Testing and Materials, 1968. Pp. 183-217.

15. Metcalfe, A. G., and M. J. Klein. "Effect of Interface on Longitudinal Tensile Properties," Composite Materials - Volume 1, Interfaces in Metal Matrix Composites. A. G. Metcalfe, editor. New York: Academic Press, Inc., 1974. Pp. 125-168.

16. Pattnaik, A., and A. Lawley. "Effect of Elevated Temperature Exposure on the Structure, Stability, and Mechanical Behavior of Aluminum-Stainless Steel Composites," Metallurgical Transactions, 5:111-122, January, 1974.

17. Forrest, J. D., and J. L. Christian. "Development and Application of High Matrix Strength Aluminum-Boron," Metals Engineering Quarterly, 10:1-6, January, 1970.

18. Chen, P. E., and J. M. Lin. "Transverse Properties of Fibrous Composites," Materials Research and Standards, 9:29-33, 1969.

19. Adams, D. F. "Inelastic Analysis of a Unidirectional Composite Subject to Transverse Normal Loading," Journal of Composite Materials, 4:310-328, 1970.

20. Cooper, G. A., and A. Kelly. "Role of the Interface in the Fracture of Fiber-Composite Materials," Interfaces in Composites. ASTM Special Technical Publication No. 452. Philadelphia: American Society for Testing and Materials, 1968. Pp. 90-106.

21. Paton, W., and A. Lockhart. "Factors Affecting the Transverse Strength of Fiber-Reinforced Metals," National Engineering Laboratory Report 475, Glasgow, Scotland, 1971.

22. Kelly, A. Strong Solids. Oxford: Clarendon Press, 1966.

23. Daniels, H. E. "The Statistical Theory of the Strength of Bundles of Threads," Proceedings of the Royal Society, 183:405-435, 1945.

24. Coleman, B. D. "On the Strength of Classical Fibres and Fibre Bundles," Journal of the Mechanics and Physics of Solids, 7:60-70, November, 1958.

25. Corten, H. T. "Micromechanics and Fracture Behavior of Composites," Modern Composite Materials. L. J. Broutman and R. H. Krock, editors. Reading, Massachusetts: Addison-Wesley Publishing Company, Inc., 1967. Pp. 27-105.

26. Rosen, B. W. "Mechanics of Composite Strengthening," Fiber Composite Materials. Metals Park, Ohio: American Society for Metals, 1965. Pp. 37-75.

27. Rosen, B. W. "Strength of Uniaxial Fibrous Composites," Proceedings of the Fifth Symposium on Naval Structural Mechanics. F. W. Wendt, H. Liebowitz, and N. Perrone, editors. New York: Pergamon Press, 1970. Pp. 621-651.

28. Rosen, B. W. "Tensile Failure of Fibrous Composites," AIAA Journal, 2:1985-1991, November, 1964.

29. Rosen, B. W., F. D. Norris, and Z. Hashin. "Mechanical Properties of Fibrous Composites," National Aeronautics and Space Administration CR-31, Washington, D. C., April, 1964.

30. Bolz, R. E., and G. L. Tuve (editors). Handbook of Tables for Applied Engineering Science. Cleveland, Ohio: The Chemical Rubber Company, 1970.

31. Wills, J. L. "The Effects of Thermal Cycling on Boron-Aluminum Composites." Unpublished Master's thesis, The University of Tennessee, Knoxville, 1972.

32. Kennedy, A. J. Processes of Creep and Fatigue in Metals. New York: John Wiley and Sons, Inc., 1963.

33. Taira, S. "Thermal Fatigue and Its Relation to Creep Rupture and Mechanical Fatigue," High Temperature Structures and Materials--Proceedings of the Third Symposium on Naval Structural Mechanics. A. M. Freudenthal, B. A. Boley, and H. Liebowitz, editors. New York: Pergamon Press, 1964. Pp. 187-213.

34. Taira, S., M. Ohnami, H. Minata, and T. Shiraishi. "Thermal Fatigue and Cyclic Mechanical Strain Fatigue at Elevated Temperature of 18-8 Cb Stainless Steel and 2125 Cr-1 Mo Steel," Bulletin of JSME, 6:169-177, 1963.

35. Ellison, E. G. "A Review of the Interaction of Creep and Fatigue," Journal of Mechanical Engineering Science, 11:318-339, March, 1969.

36. McClintock, F. A., and A. S. Argon. Mechanical Behavior of Materials. Reading, Massachusetts: Addison-Wesley Publishing Company, Inc., 1966.

37. Wright, M. A. "The Effect of Thermal Cycling on the Mechanical Properties of Various Aluminum Alloys Reinforced with Unidirectional Boron Fibers," Metallurgical Transactions, 6A:129-134, January, 1975.

38. Shahanian, P. "Thermal Fatigue of Boron-Aluminum Composites," SAMPE Quarterly, 2:28-35, June, 1970.

39. Kreider, K. G., and V. M. Patarini. "Thermal Expansion of Boron Fiber-Aluminum Composites," Metallurgical Transactions, 1:3431-3435, December, 1970.

40. Turner, P. S. "Thermal-Expansion Stresses in Reinforced Plastics," Journal of Research, 37:239-250, October, 1946.

41. Thomas, J. P. "The Effect of Inorganic Filler on the Coefficient of Thermal Expansion of Polymeric Materials," Convair Report No. FGT-2713 prepared by General Dynamics, Inc., Fort Worth, Texas, December, 1960.

42. Finnie, I., and W. R. Heller. Creep of Engineering Material. New York: McGraw-Hill Book Company, Inc., 1959.

43. Dieter, G. E. Mechanical Metallurgy. Metallurgy and Metallurgical Engineering Series, R. F. Mehl and M. B. Bever, editors. New York: McGraw-Hill Book Company, Inc., 1961.

44. Prewo, K. M. "Anelastic Creep of Boron Fibers," Journal of Composite Materials, 8:411-414, October, 1974.

45. Ericksen, R. H. "Room Temperature of Borsic-Aluminum Composites," Metallurgical Transactions, 4:1687-1693, July, 1973.

46. Toth, I. J. "Creep and Fatigue Behavior of Unidirectional and Cross-Plied Composites," Composite Materials: Testing and Design. ASTM Special Technical Publication No. 460. Philadelphia: American Society for Testing and Materials, 1969. Pp. 236-253.

47. Breinan, E. M., and K. G. Kreider. "Axial Creep and Stress-Rupture of B-Al Composites," Metallurgical Transactions, 1:93-104, January, 1970.

48. Pinnel, M. R., and A. Lawley. "Correlation of Creep Elongation and Substructure in Aluminum Stainless Steel Composites," Metallurgical Transactions, 2:1415-1422, May, 1971.

49. Breinan, E. M., and K. G. Kreider. "Transverse Creep and Stress-Rupture of Borsic-Aluminum Composites and Borsic-Aluminum Composites Containing Stainless Steel and Titanium," Metallurgical Transactions, 4:1155-1165, April, 1973.

50. Reed-Hill, R. E. Physical Metallurgy Principles. Cincinnati, Ohio: D. Van Nostrand Company, 1973.

51. Wright, M. A. "The Mechanical Properties of Metal Matrix Composites Subjected to Cyclic Temperature Changes." Technical Report prepared under Navy Contract No. N0014-71-A-0121-0003 NR 031-760 by The University of Tennessee Space Institute, Tullahoma, Tennessee, October, 1974.

52. Allred, R. E., W. R. Hoover, and J. A. Horak. "Elastic-Plastic Poisson's Ratio of Borsic-Aluminum," Journal of Composite Materials, 8:15-37, 1974.

53. White, M. Private communication. The University of Tennessee Space Institute, Tullahoma, Tennessee, 1975.

54. Wright, M. A. "The Effect of Elevated Temperatures on the Structural Properties of Fiber Composite Materials Suitable for Use in Space Shuttle and Other Space Vehicles." Report prepared under NASA Contract No. UT 844001-6463R-95 by The University of Tennessee Space Institute, Tullahoma, Tennessee, December, 1971.

55. Sessler, J. G., and V. Weiss. Aerospace Structural Metals Handbook, Volume II - Nonferrous Light Metal Alloys. Wright-Patterson Air Force Base, Ohio: Air Force Materials Laboratory, Air Force Systems Command, 1968.

APPENDIX

TABLE I

THE EFFECT OF THERMAL CYCLING ON MECHANICAL PROPERTIES OF STAINLESS STEEL REINFORCED ALUMINUM ALLOY

	σ_{UTS} (ksi)	E ($\times 10^6$ psi)	ρ (gm/cm^3)
As-received			
(a) 1972 Panel	241.05	16.73	4.987
(b) 1973 Panel	146.11	16.02	5.023
(c) Transverse Section	18.13	13.56	4.877
3 Minutes/Cycle			
(a) 1972 Panel	194.86	14.20	4.876
(b) Transverse Section	11.76	11.61	4.954
6 Minutes/Cycle			
(a) 1973 Panel	128.82	14.39	4.921
12 Minutes/Cycle			
(b) 1973 Panel	131.49	13.34	4.949

TABLE II

THE EFFECT OF THERMAL CYCLING ON MECHANICAL PROPERTIES OF SILICON-CARBIDE REINFORCED ALUMINUM ALLOY

	σ_{UTS}(ksi)	E(x 10^6 psi)	ρ(gm/cm^3)
As-received			
(a) 1972 Panel	81.00	29.35	3.008
(b) 1973 Panel	84.71	30.05	3.010
(c) Transverse Section	20.88	24.12	2.977
3 Minutes/Cycle			
(a) 1972 Panel	70.66	28.04	2.815
(b) Transverse Section	11.42	17.17	2.991
6 Minutes/Cycle			
(a) 1973 Panel	54.05	19.35	2.901
12 Minutes/Cycle			
(a) 1973 Panel	58.62	18.46	2.729

TABLE III

THE EFFECT OF THERMAL CYCLING ON MECHANICAL PROPERTIES OF UNIDIRECTIONAL BORON REINFORCED ALUMINUM ALLOY

	σ_{UTS} (ksi)	E (x 10^6 psi)	ρ (gm/cm^3)
As-received			
(a) 1972 Panel	130.53	22.70	2.670
(b) 1973 Panel	128.07	21.20	2.639
(c) Transverse Section	29.26	16.04	2.652
3 Minutes/Cycle			
(a) 1972 Panel	80.04	22.10	2.704
(b) Transverse Section	16.38	15.52	2.728
6 Minutes/Cycle			
(a) 1973 Panel	48.94	21.00	2.688
(b) Transverse Section	14.42	12.86	2.704
12 Minutes/Cycle			
(a) 1973 Panel	26.17	14.41	2.721
Fully Annealed			
1973 Panel	121.11	20.74	2.633

TABLE IV

THE EFFECT OF THERMAL CYCLING ON MECHANICAL PROPERTIES OF 0° TO 90° CROSSPLIED BORON REINFORCED ALUMINUM ALLOY

	σ_{UTS} (ksi)	E (x 10^6 psi)	ρ (gm/cm^3)
As-received			
(a) 1972 Panel	102.60	18.41	2.690
(b) 1973 Panel	111.73	18.98	2.628
3 Minutes/Cycle			
(a) 1972 Panel	66.40	13.97	2.128
6 Minutes/Cycle			
(a) 1973 Panel	33.10	12.32	2.461
12 Minutes/Cycle			
(a) 1973 Panel	10.78	12.42	2.410

TABLE V

THE EFFECT OF THERMAL CYCLING ON MECHANICAL PROPERTIES OF ±45° CROSSPLIED BORON REINFORCED ALUMINUM ALLOY

	σ_{UTS}(ksi)	E(x 10^6 psi)	ρ(gm/cm^3)
As-received	36.57	14.292	2.639
3 Minutes/Cycle	24.95	8.778	2.642
6 Minutes/Cycle	10.80	6.520	2.443
12 Minutes/Cycle	10.09	4.613	2.491

TABLE VI

THE RELATIVE THERMAL EXPANSION OF A BORON-ALUMINUM COMPOSITE SUBJECTED TO THERMAL CYCLING USING A THREE-MINUTE PERIOD

Time (sec)	$(\Delta L/L_o)_{Al} - (\Delta L/L_o)_{B-Al}$ ($\times 10^{-3}$ inch/inch)							
	10	50	500	1400	2000	3300	4900	6000
0	0.000	0.000	0.000	0.000	0.000	0.000	0.000	0.000
10	-0.277	-0.149	-0.181	0.000	-0.096	-0.023	-0.004	-0.048
20	-0.015	0.153	0.164	0.219	0.173	0.216	0.226	0.221
30	0.198	0.362	0.402	0.365	0.332	0.381	0.440	0.440
40	0.473	0.621	0.700	0.592	0.592	0.620	0.731	0.738
50	0.745	0.877	0.966	0.832	0.851	0.868	1.015	1.011
60	1.049	1.167	1.271	1.176	1.163	1.167	1.322	1.315
70	1.365	1.483	1.637	1.479	1.530	1.490	1.650	1.665
80	1.698	1.843	2.042	1.885	1.937	1.902	2.020	2.047
90	2.033	2.194	2.695	2.294	2.348	2.308	2.393	2.444
100	2.204	2.280	2.529	2.397	2.433	2.356	2.453	2.511
110	1.909	1.899	2.231	2.147	2.217	2.188	2.253	2.286
120	1.551	1.545	1.953	1.935	1.986	1.959	2.006	2.025
130	1.174	1.190	1.623	1.629	1.662	1.642	1.617	1.663
140	0.893	0.930	1.306	1.330	1.352	1.327	1.315	1.329
150	0.648	0.695	0.960	1.018	1.018	0.990	0.975	1.002
160	0.433	0.478	0.630	0.695	0.698	0.655	0.653	0.672
170	0.225	0.249	0.304	0.368	0.359	0.340	0.317	0.347
180	0.043	0.055	0.033	0.073	0.058	0.044	0.041	0.047

TABLE VII

THE RELATIVE THERMAL EXPANSION OF A BORON-ALUMINUM COMPOSITE SUBJECTED TO THERMAL CYCLING USING A SIX-MINUTE PERIOD

Time (sec)	$(\Delta L/L_o)_{Al} - (\Delta L/L_o)_{B-Al}$ ($\times 10^{-3}$ inch/inch)						
	10	50	600	1000	2200	4000	6000
0	0.000	0.000	0.000	0.000	0.000	0.000	0.000
10	0.029	0.223	0.125	0.186	0.224	0.181	0.158
20	0.468	0.618	0.515	0.581	0.593	0.504	0.500
30	0.803	0.882	0.759	0.825	0.847	0.745	0.756
40	1.090	1.157	0.986	1.035	1.046	0.956	0.960
50	1.364	1.370	1.214	1.275	1.256	1.186	1.187
60	1.617	1.619	1.450	1.538	1.509	1.431	1.424
70	1.832	1.849	1.673	1.762	1.751	1.670	1.635
80	2.119	2.169	1.997	2.080	2.082	1.993	1.941
90	2.452	2.502	2.350	2.438	2.444	2.374	2.285
100	2.761	2.807	2.681	2.779	2.765	2.718	2.587
110	3.039	3.079	2.978	3.084	3.075	3.002	2.874
120	3.258	3.314	3.241	3.343	3.330	3.260	3.119
130	3.581	3.621	3.556	3.674	3.652	3.574	3.425
140	3.869	3.950	3.876	4.000	3.981	3.892	3.730
150	4.127	4.202	4.139	4.270	4.249	4.158	3.987
160	4.383	4.406	4.383	4.520	4.491	4.402	4.217
170	4.622	4.663	4.623	4.762	4.739	4.645	4.507
180	4.821	4.863	4.855	4.976	4.955	4.853	4.712

TABLE VII (continued)

Time (sec)	$(\Delta L/L_o)_{Al} - (\Delta L/L_o)_{B-Al}$ (x 10^{-3} inch/inch)						
	10	50	600	1000	2200	4000	6000
190	4.940	4.816	4.889	4.949	4.947	4.814	4.593
200	4.711	4.678	4.768	4.857	4.842	4.765	4.561
210	4.535	4.608	4.693	4.805	4.782	4.727	4.530
220	4.354	4.470	4.567	4.664	4.656	4.612	4.421
230	4.124	4.250	4.346	4.435	4.429	4.411	4.229
240	3.868	3.987	4.079	4.163	4.158	4.150	3.980
250	3.569	3.679	3.775	3.849	3.835	3.820	3.685
260	3.244	3.366	3.437	3.500	3.486	3.500	3.348
270	2.915	3.014	3.088	3.143	3.128	3.145	2.997
280	2.582	2.672	2.727	2.775	2.774	2.783	2.653
290	2.246	2.318	2.356	2.394	2.403	2.403	2.305
300	1.899	1.961	1.999	2.013	2.026	2.032	1.933
310	1.565	1.619	1.638	1.651	1.668	1.661	1.585
320	1.225	1.295	1.339	1.291	1.312	1.302	1.241
330	0.861	0.907	0.916	0.888	0.920	0.909	0.869
340	0.587	0.623	0.622	0.598	0.624	0.606	0.581
350	0.283	0.307	0.283	0.278	0.295	0.283	0.273
360	-0.010	-0.002	-0.011	-0.009	0.007	-0.008	-0.009

TABLE VIII

THE RELATIVE THERMAL EXPANSION OF A BORON-ALUMINUM COMPOSITE SUBJECTED TO THERMAL CYCLING USING A TWELVE-MINUTE PERIOD

Time (sec)	$(\Delta L/L_o)_{Al} - (\Delta L/L_o)_{B-Al}$ ($\times 10^{-3}$ inch/inch)								
	20	100	400	1200	2100	2900	4100	5100	6000
0	0.000	0.000	0.000	0.000	0.000	0.000	0.000	0.000	0.000
10	0.286	0.347	0.222	0.335	0.305	0.258	0.289	0.295	0.314
20	0.693	0.760	0.645	0.753	0.699	0.658	0.698	0.660	0.679
30	1.029	1.121	0.989	1.086	1.025	0.991	1.038	0.965	0.985
40	1.353	1.458	1.334	1.398	1.358	1.323	1.364	1.275	1.288
50	1.668	1.775	1.638	1.697	1.655	1.641	1.667	1.555	1.576
60	2.019	2.130	1.981	2.033	1.986	1.983	2.007	1.887	1.910
70	2.270	2.371	2.212	2.263	2.229	2.238	2.242	2.111	2.142
80	2.552	2.654	2.483	2.525	2.518	2.532	2.514	2.387	2.419
90	3.817	2.921	2.743	2.770	2.783	2.812	2.779	2.646	2.682
100	3.080	3.191	3.008	3.023	3.054	3.087	3.053	2.910	2.939
110	3.327	3.473	3.260	3.314	3.310	3.350	3.304	3.155	3.190
120	3.563	3.724	3.511	3.552	3.554	3.607	3.542	3.394	3.423
130	3.793	3.979	3.753	3.767	3.793	3.848	3.775	3.621	3.661
140	4.031	4.224	3.981	3.988	4.027	4.086	3.999	3.844	3.879
150	4.251	4.453	5.194	4.201	4.241	4.305	4.209	4.045	4.081
160	4.459	4.672	4.404	4.394	4.448	4.507	4.399	4.238	4.275
170	4.654	4.881	4.601	4.576	4.621	4.700	4.575	4.405	4.447

TABLE VIII (continued)

Time (sec)	$(\Delta L/L_o)_{Al} - (\Delta L/L_o)_{B\text{-}Al}$ (x 10^{-3} inch/inch)								
	20	100	400	1200	2100	2900	4100	5100	6000
180	4.849	5.085	4.796	4.749	4.797	4.882	4.746	4.585	4.617
190	5.020	5.280	4.978	4.908	4.960	5.053	4.904	4.732	4.773
200	5.191	5.462	5.145	5.056	5.109	5.212	5.052	4.876	4.919
210	5.345	5.614	5.299	5.187	5.248	5.357	5.182	5.013	5.051
220	5.497	5.770	5.453	5.326	5.385	5.498	5.323	5.137	5.181
230	5.644	5.919	5.595	5.458	5.514	5.634	5.449	5.259	5.305
240	5.700	5.982	5.650	5.511	5.563	5.684	5.491	5.299	5.346
250	5.895	6.190	5.853	5.710	5.761	5.881	5.676	5.491	5.535
260	6.025	6.326	5.984	5.841	5.886	6.001	5.797	5.607	5.648
270	6.146	6.453	6.102	5.970	6.000	6.117	5.903	5.714	5.753
280	6.248	6.565	6.207	6.084	6.102	6.217	5.997	5.807	5.841
290	6.331	6.653	6.291	6.183	6.184	6.297	6.074	5.886	5.917
300	6.483	6.809	6.438	6.349	6.327	6.443	6.212	6.025	6.049
310	6.601	6.927	6.550	6.480	6.438	6.554	6.320	6.133	6.155
320	6.710	7.047	6.660	6.596	6.544	6.662	6.420	6.234	6.250
330	6.818	7.152	6.765	6.710	6.651	6.774	6.522	6.335	6.353
340	6.919	7.256	6.866	6.822	6.744	6.872	6.614	6.429	6.440
350	7.015	7.352	6.962	6.926	6.844	6.973	6.708	6.523	6.531

TABLE VIII (continued)

Time (sec)	$(\Delta L/L_o)_{Al} - (\Delta L/L_o)_{B\text{-}Al}$ (x 10^{-3} inch/inch)								
	20	100	400	1200	2100	2900	4100	5100	6000
360	7.070	7.414	7.023	6.990	6.905	7.035	6.763	6.578	6.585
370	7.112	7.342	7.116	6.968	6.999	7.171	6.859	6.701	6.636
380	6.898	7.198	6.949	6.896	6.910	7.079	6.798	6.644	6.632
390	6.550	6.878	6.631	6.662	6.622	6.794	6.557	6.396	6.415
400	6.395	6.740	6.501	6.599	6.508	6.690	6.483	6.333	6.357
410	6.072	6.425	6.189	6.344	6.211	6.409	6.219	6.079	6.101
420	5.739	6.068	5.831	6.040	5.874	6.080	5.908	5.771	5.791
430	5.402	5.708	5.474	5.699	5.516	5.731	5.567	5.442	5.455
440	5.069	5.340	5.086	5.327	5.130	5.341	5.205	5.075	5.087
450	4.773	4.985	4.714	4.956	4.763	4.968	4.841	4.726	4.732
460	4.477	4.623	4.343	4.611	4.383	4.598	4.505	4.369	4.369
470	4.174	4.253	3.984	4.258	4.024	4.229	4.136	4.025	4.023
480	3.854	3.884	3.629	3.896	3.654	3.649	3.781	3.668	3.484
490	3.500	3.536	3.291	3.546	3.302	3.486	3.443	3.335	3.320
500	3.163	3.193	2.953	3.194	2.955	3.143	3.114	3.002	2.987
510	2.844	2.862	2.614	2.851	2.622	2.801	2.774	2.668	2.664
520	2.525	2.519	2.284	2.516	2.296	2.466	2.442	2.349	2.330
530	2.199	2.196	1.966	2.199	1.998	2.146	2.121	2.043	2.014

TABLE VIII (continued)

Time (sec)	$(\Delta L/L_o)_{Al} - (\Delta L/L_o)_{B-Al}$ (x 10^{-3} inch/inch)								
	20	100	400	1200	2100	2900	4100	5100	6000
540	1.915	1.895	1.693	1.911	1.726	1.870	1.833	1.762	1.739
550	1.644	1.632	1.447	1.645	1.483	1.621	1.574	1.508	1.481
560	1.407	1.385	1.223	1.406	1.265	1.390	1.333	1.283	1.259
570	1.157	1.171	1.020	1.189	1.070	1.183	1.121	1.074	1.062
580	0.970	0.956	0.828	0.983	0.880	0.976	0.909	0.882	0.862
590	0.818	0.801	0.692	0.840	0.743	0.834	0.762	0.746	0.721
600	0.667	0.655	0.559	0.688	0.605	0.689	0.621	0.603	0.586
610	0.541	0.527	0.449	0.568	0.489	0.558	0.497	0.488	0.466
620	0.428	0.417	0.347	0.451	0.380	0.449	0.384	0.394	0.362
630	0.335	0.325	0.268	0.359	0.295	0.353	0.294	0.294	0.278
640	0.295	0.237	0.186	0.266	0.208	0.261	0.205	0.209	0.196
650	0.169	0.157	0.123	0.195	0.144	0.187	0.142	0.143	0.131
660	0.108	0.107	0.079	0.136	0.098	0.130	0.887	0.093	0.081
670	0.066	0.061	0.037	0.088	0.054	0.081	0.048	0.053	0.041
680	0.035	0.027	0.014	0.054	0.025	0.045	0.016	0.023	0.015
690	0.007	0.001	0.009	0.022	0.001	0.015	0.004	-0.003	-0.005
700	-0.013	-0.017	-0.025	-0.001	-0.016	-0.005	-0.011	-0.017	-0.020
710	-0.023	-0.026	-0.027	-0.019	-0.023	-0.017	-0.020	-0.025	-0.024
720	-0.031	-0.030	-0.030	-0.030	-0.030	-0.030	-0.030	-0.030	-0.030

TABLE IX

THE THEORETICAL AND EXPERIMENTAL COMPOSITE STRENGTH AS OBTAINED FOR AS-RECEIVED AND THERMALLY CYCLED MATERIAL

Fiber Type	Condition	Lower Bound (ksi)	Upper Bound (ksi)	Actual (ksi)
SiC	As-received	78	159	86
SiC	6 Minutes Cycle	69	-	65
SiC	12 Minutes Cycle	72	-	57
B	As-received	72	121	132
B	3 Minutes Cycle	81	116	103
B	6 Minutes Cycle	39	68	45
B	12 Minutes Cycle	56	91	31

TABLE X

THE EXPERIMENTALLY DETERMINED NUMBER OF FIBERS IN A COMPOSITE

Material	Condition	Number of Fibers Internal	Number of Fibers Extracted
B-Al[a]	As-received	351	457
B-Al	12 Minutes Cycle	352	1034
B-Al[a]	12 Minutes Cycle	363	1176
SiC-Al	As-received	358	394
SiC-Al[a]	12 Minutes Cycle	352	814

[a]Subjected to a tensile test.

TABLE XI

THE THEORETICAL COMPOSITE STRENGTH AS OBTAINED FOR AS-RECEIVED AND THERMALLY CYCLED STAINLESS STEEL REINFORCED MATERIAL

Condition	Theoretical Strength (ksi)
As-received (1972)	242.0
As-received (1973)	153.8
3 Minutes Cycle	243.4

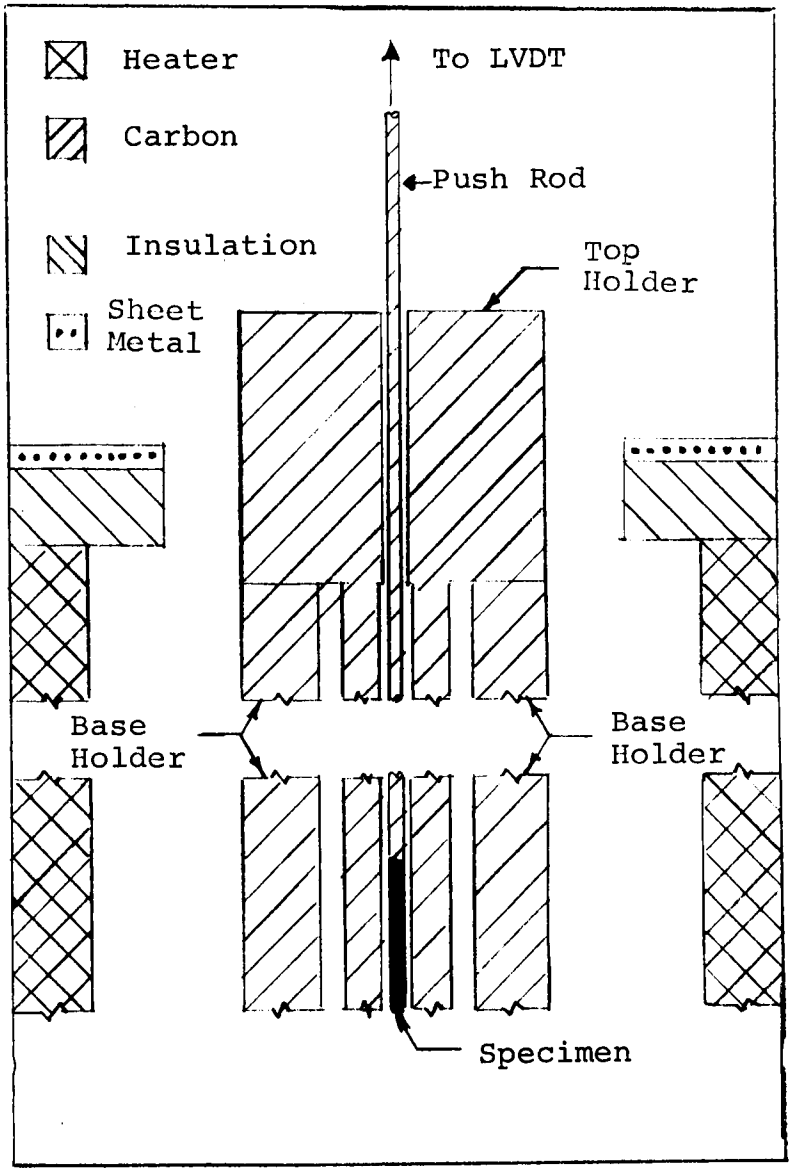

Figure 1. A diagram of the placement of a composite specimen into the dilatometer.

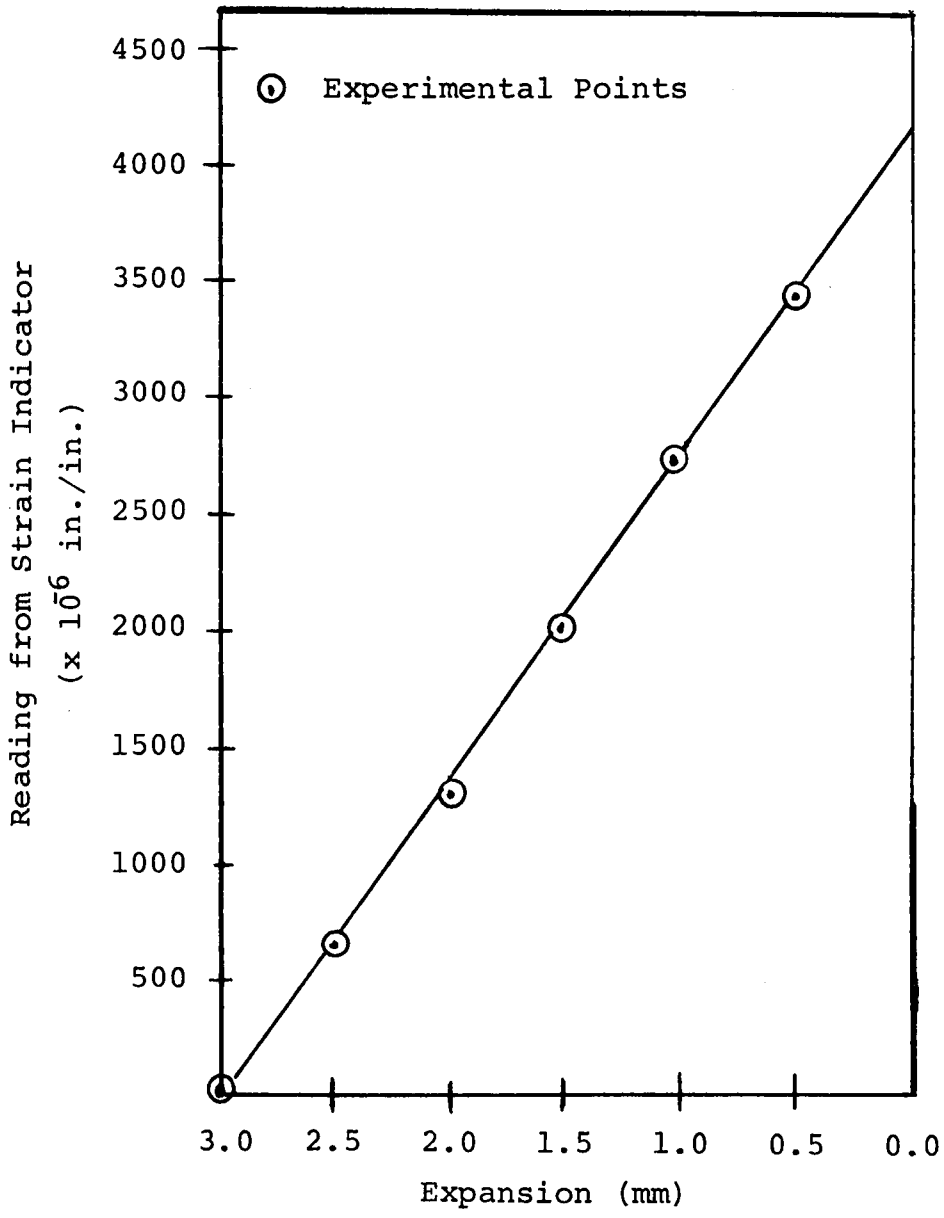

Figure 2. The calibration curve of the LVDT in the thermal expansion measurement system.

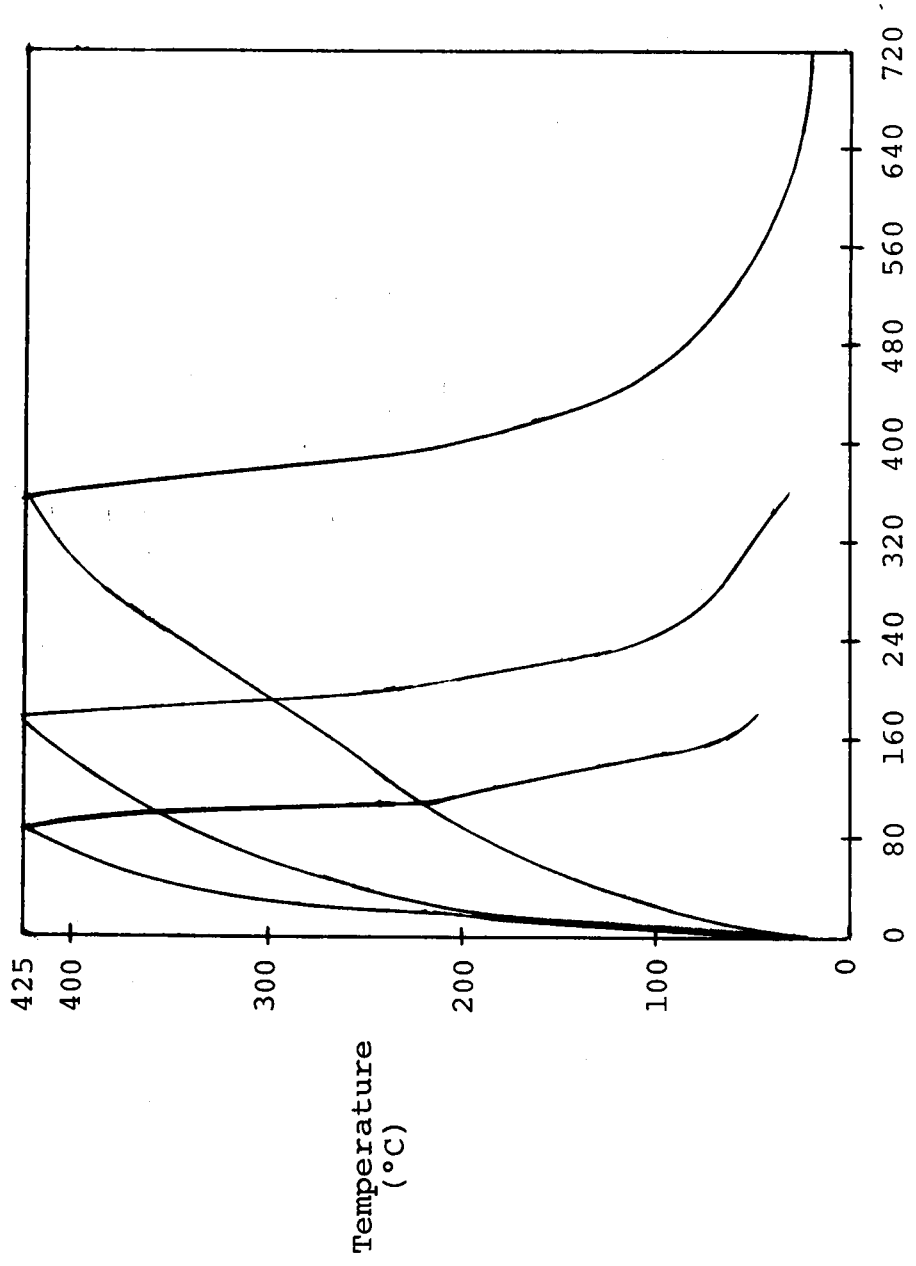

Figure 3. The temperature changes with time for specimens subjected to thermal fatigue in the dilatometer.

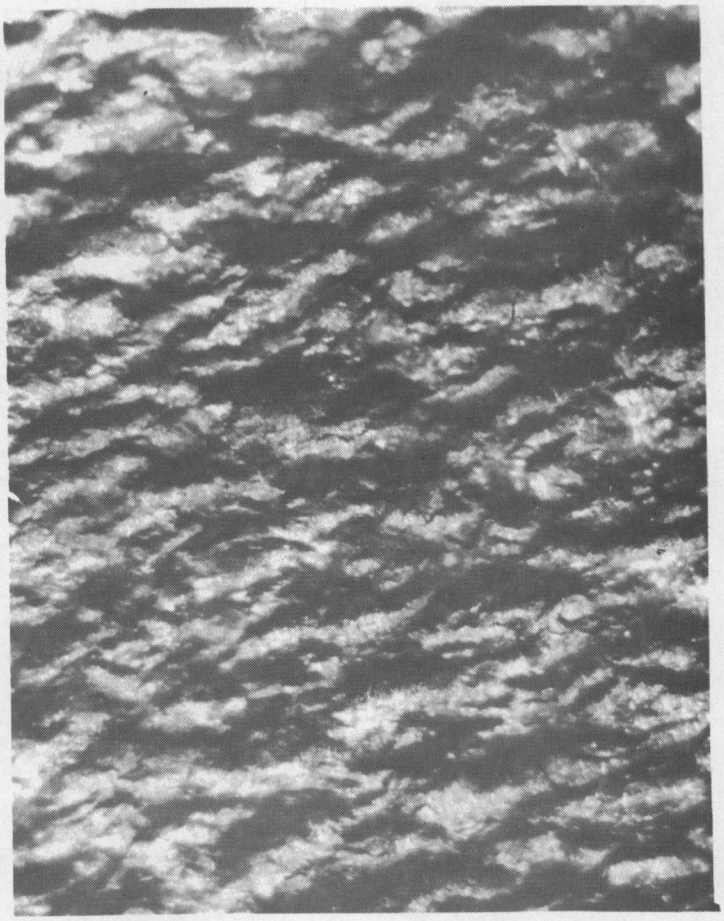

Figure 4. The surface of unidirectionally reinforced boron-aluminum after exposure to 6,000 cycles, 20°C to 425°C, three minutes per cycle; X 193.



Figure 5. The surface of unidirectionally reinforced boron-aluminum after exposure to 6,000 cycles, 20°C to 425°C, twelve minutes per cycle.

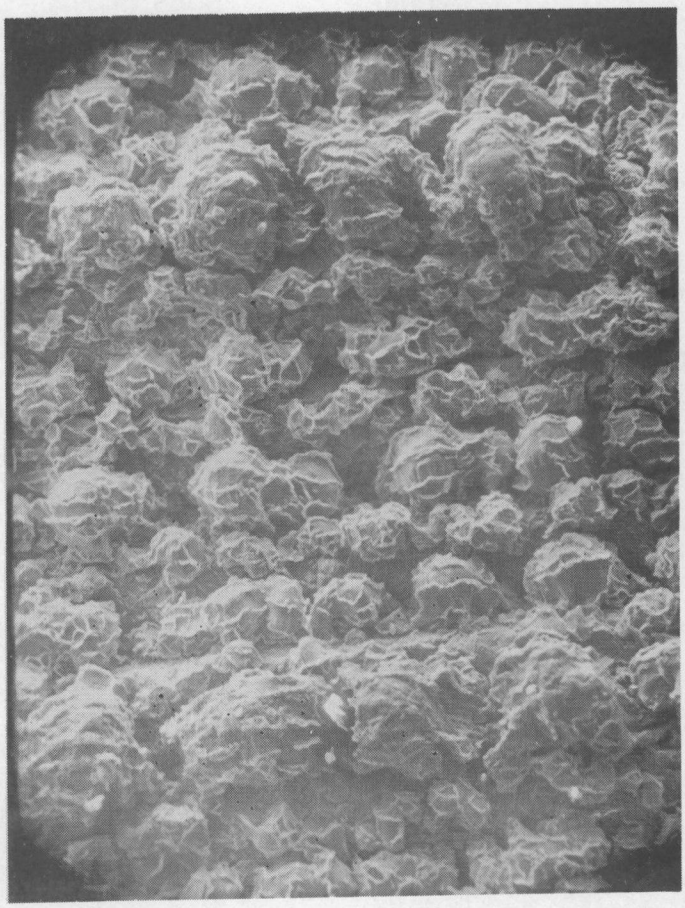

Figure 6. A Scanning Electron Micrograph showing extensive surface disruption resulting from thermal cycling using a twelve-minute period; X 100.

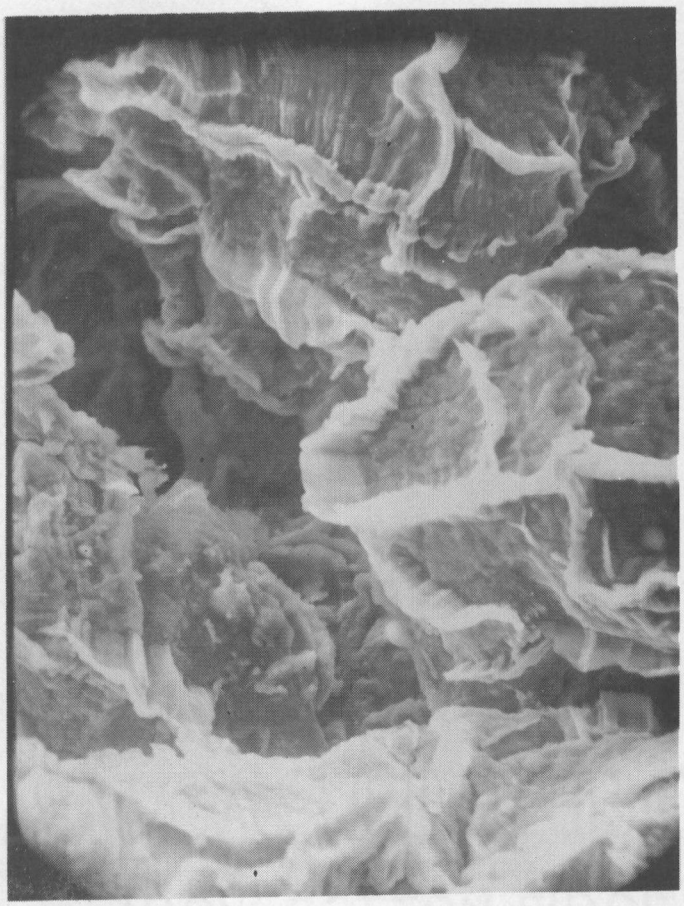

Figure 7. A Scanning Electron Micrograph showing apparent grain boundary process; X 1,000.

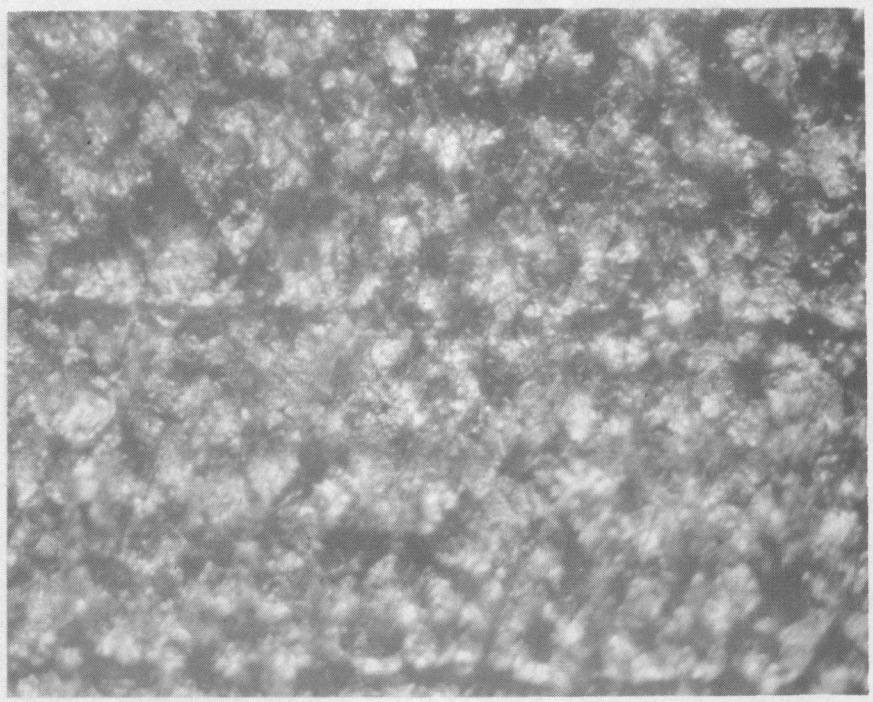

Figure 8. The surface of unidirectionally reinforced silicon carbide-aluminum after exposure to 6,000 cycles, 20°C to 425°C, three minutes per cycle; X 193.

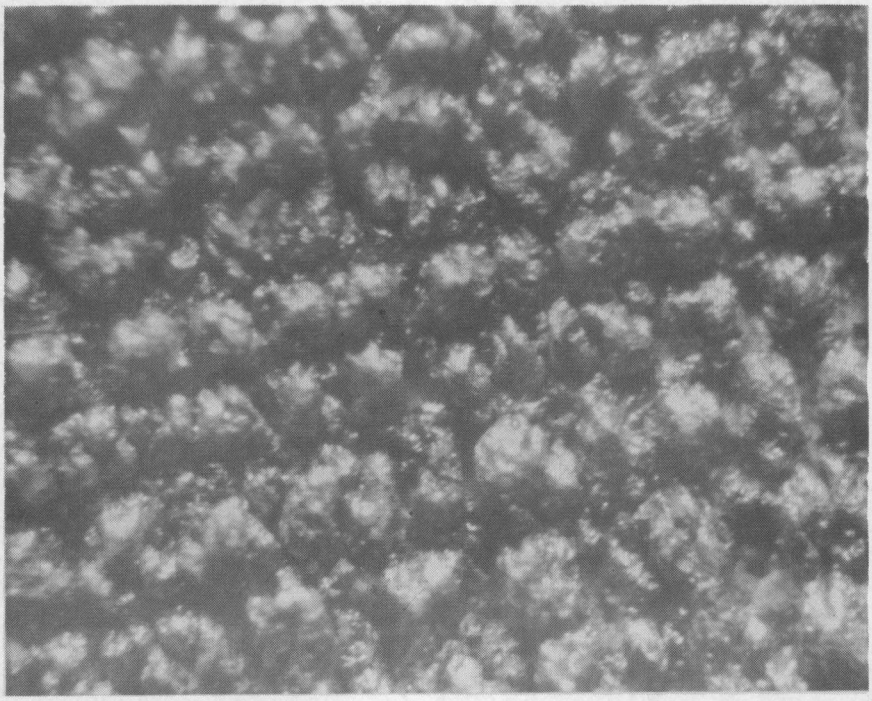

Figure 9. The surface of unidirectionally reinforced silicon carbide-aluminum after exposure to 6,000 cycles, 20°C to 425°C, six minutes per cycle; X 193.



Figure 10. The surface of unidirectionally reinforced silicon carbide-aluminum after exposure to 6,000 cycles, 20°C to 425°C, twelve minutes per cycle; X 193.

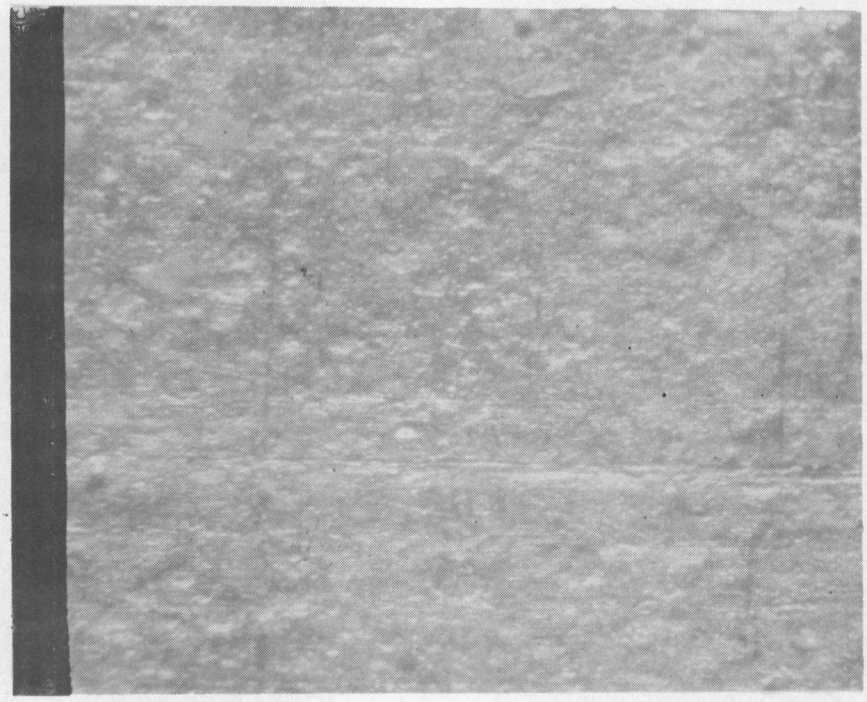

Figure 11. The surface of unidirectionally reinforced stainless steel-aluminum after exposure to 6,000 cycles, 20°C to 365°C, three minutes per cycle; X 193.

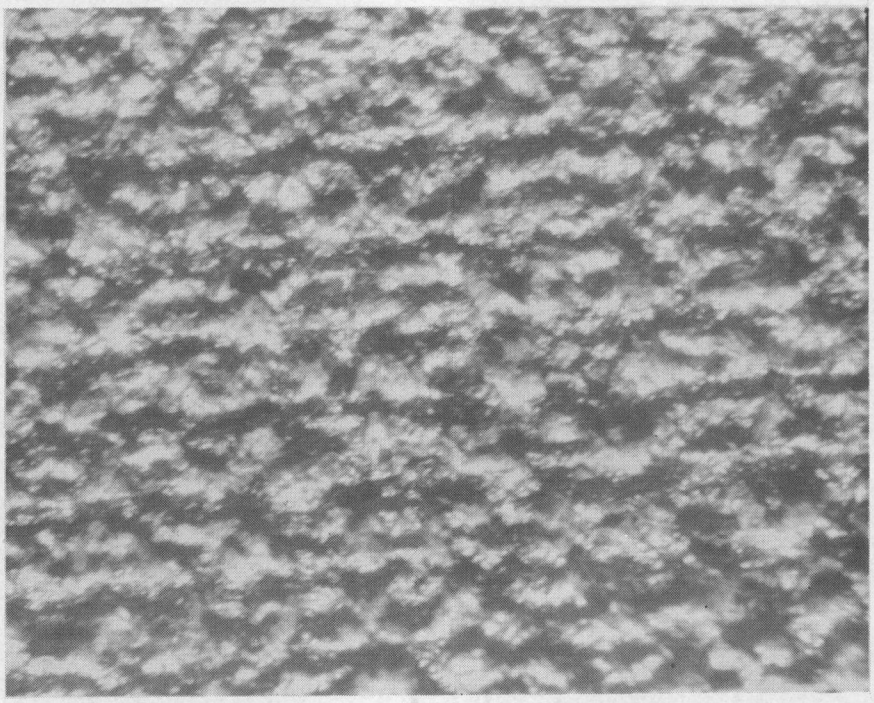

Figure 12. The surface of unidirectionally reinforced stainless steel-aluminum after exposure to 6,000 cycles, 20°C to 365°C, six minutes per cycle; X 193.



Figure 13. The surface of unidirectionally reinforced stainless steel-aluminum after exposure to 6,000 cycles, 20°C to 365°C, twelve minutes per cycle; X 193.

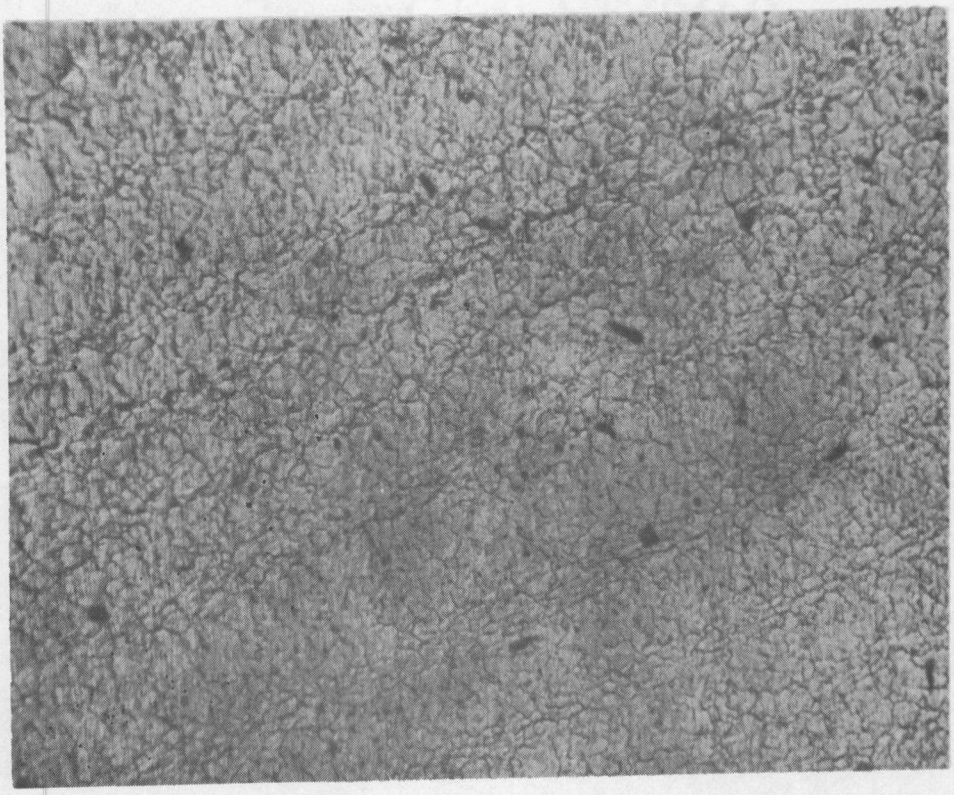

Figure 14. The surface of a boron reinforced specimen subjected to five cyclic temperature changes, 20°C to 425°C, six minutes per cycle.

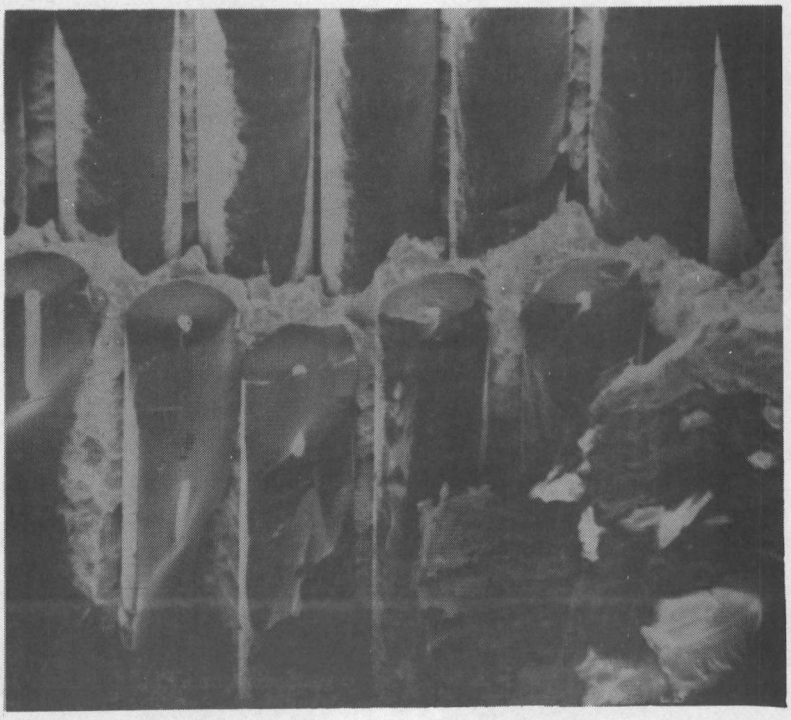

Figure 15. The internal voids in a boron reinforced specimen subjected to 6,000 thermal cycles; X 193.

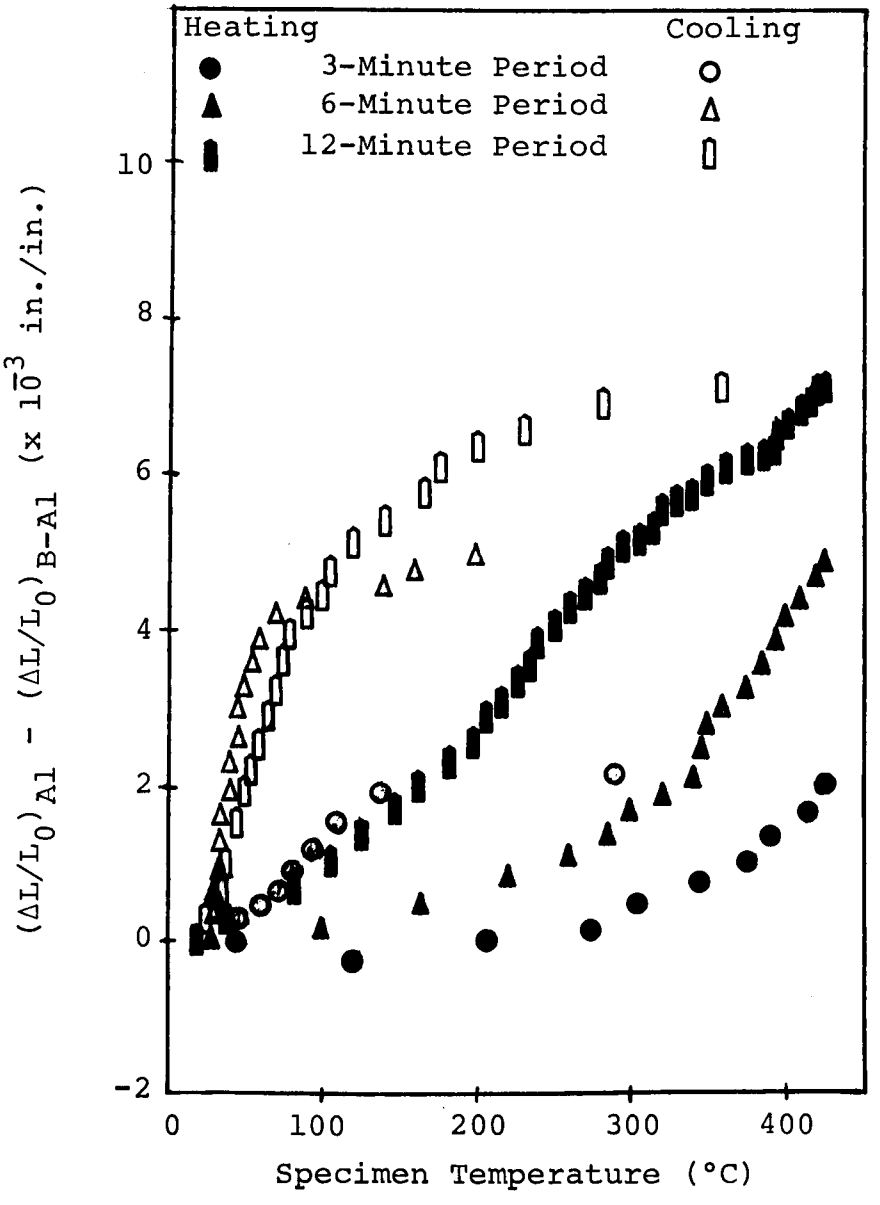

Figure 16. The thermal expansion of boron-aluminum during the tenth to twentieth thermal cycles.

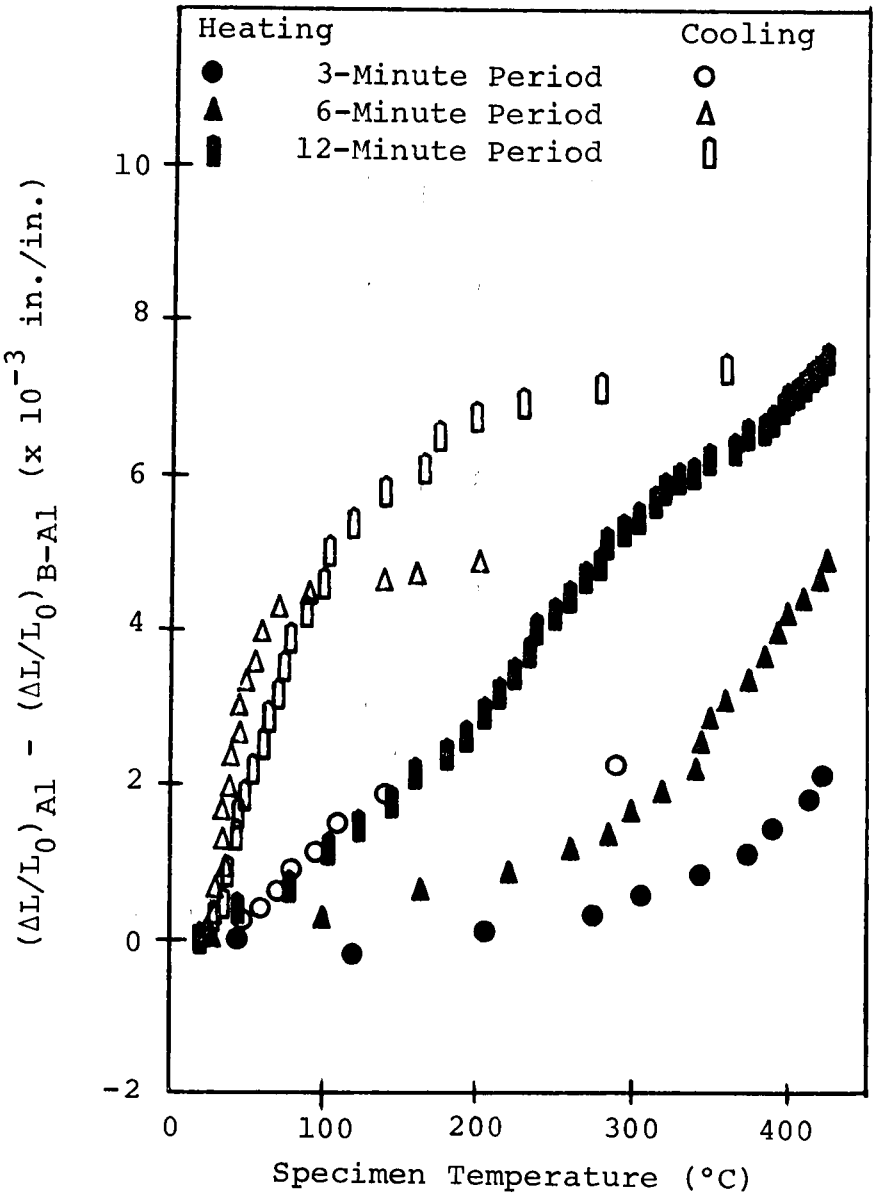

Figure 17. The thermal expansion of boron-aluminum during the fiftieth to one hundredth thermal cycles.

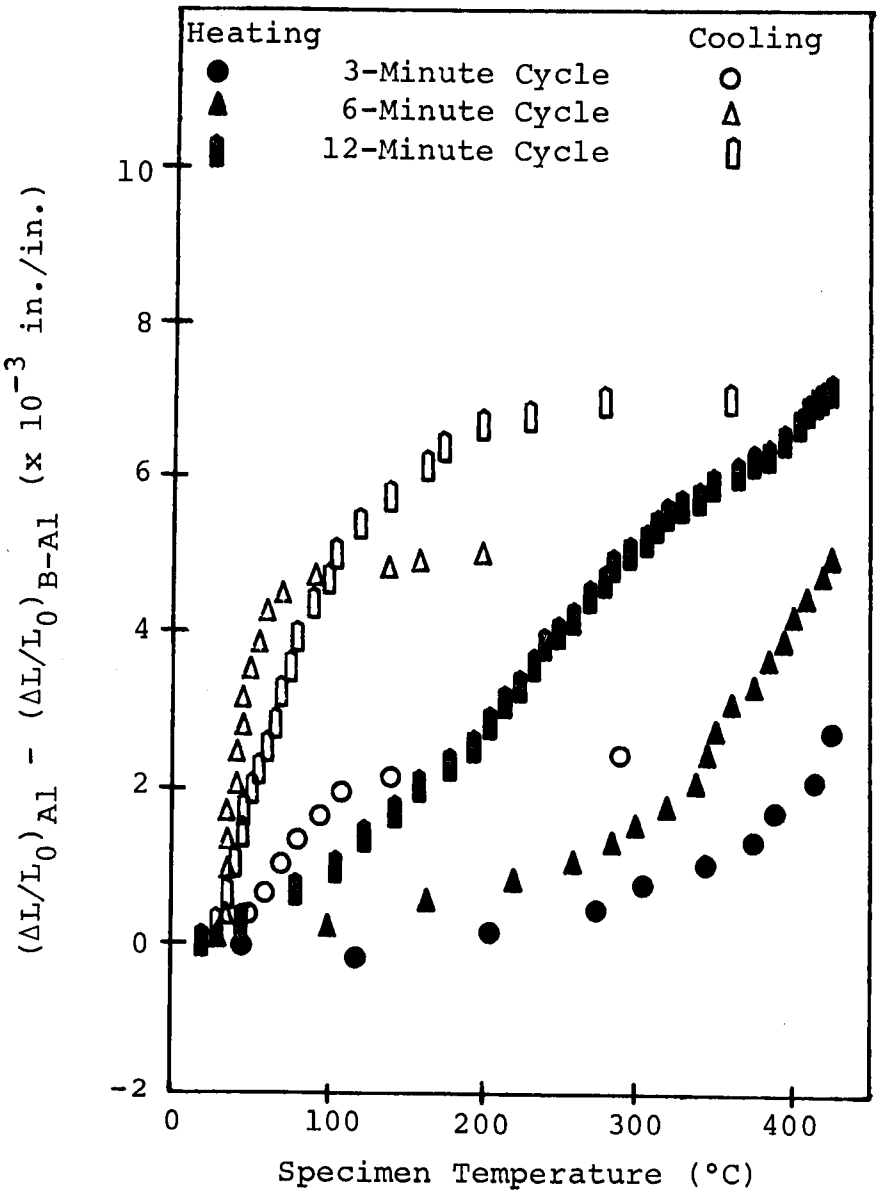

Figure 18. The thermal expansion of boron-aluminum during the four hundredth to six hundredth thermal cycles.

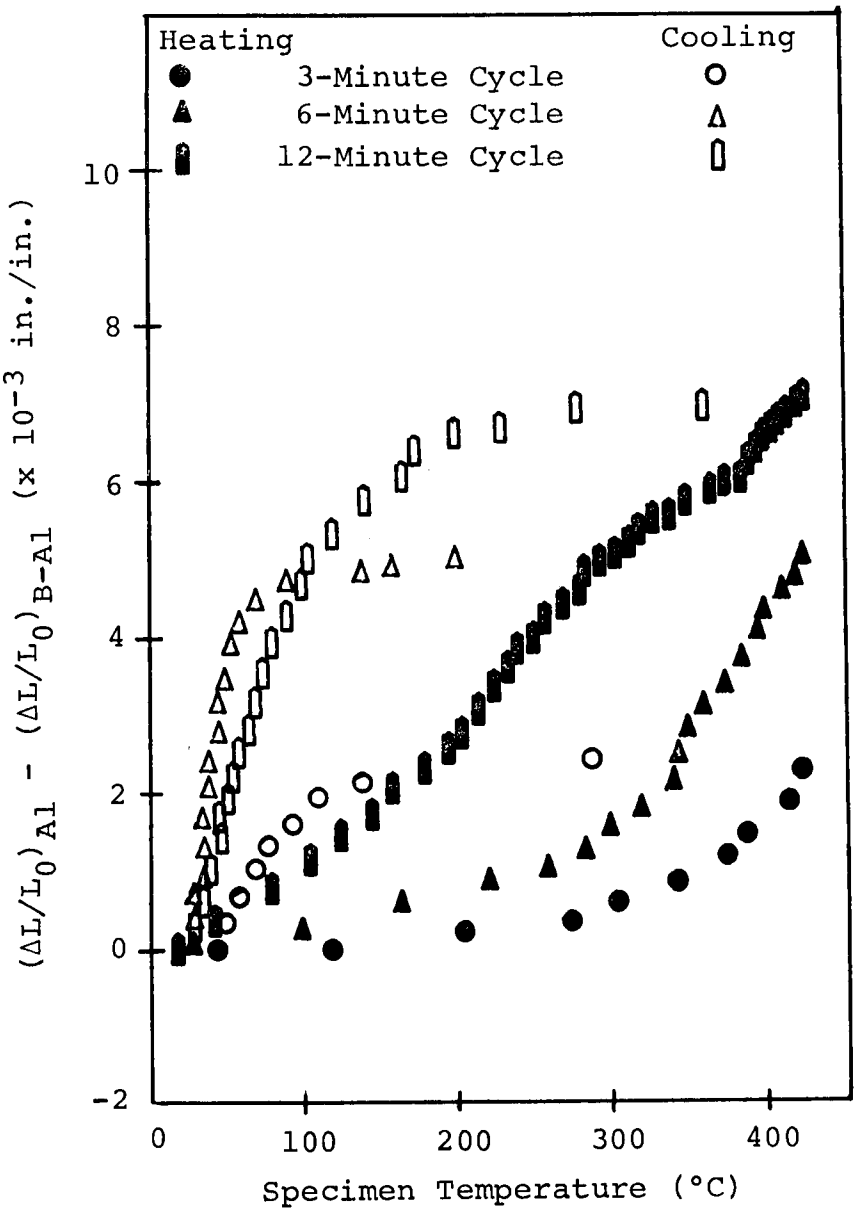

Figure 19. The thermal expansion of boron-aluminum during the one thousandth to fourteen hundredth thermal cycles.

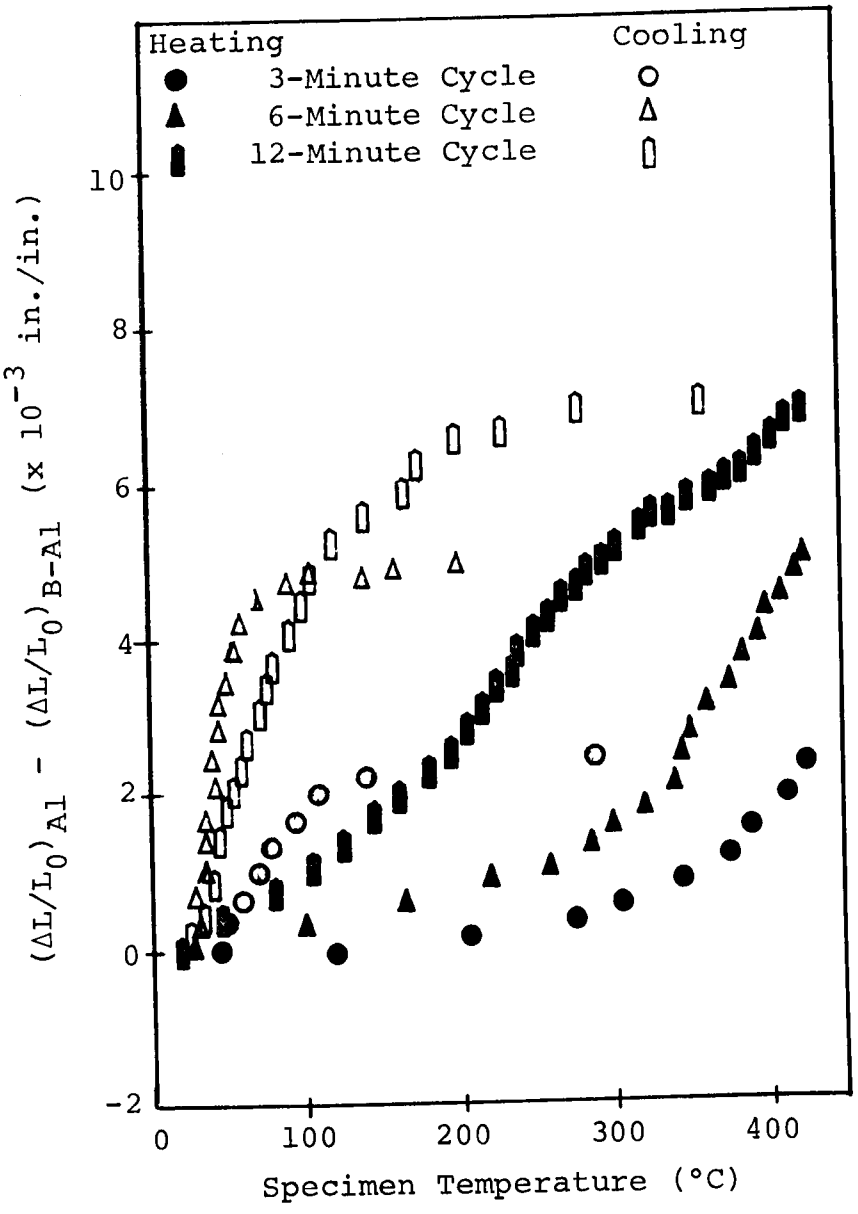

Figure 20. The thermal expansion of boron-aluminum during the two thousandth to twenty-two hundredth thermal cycles.

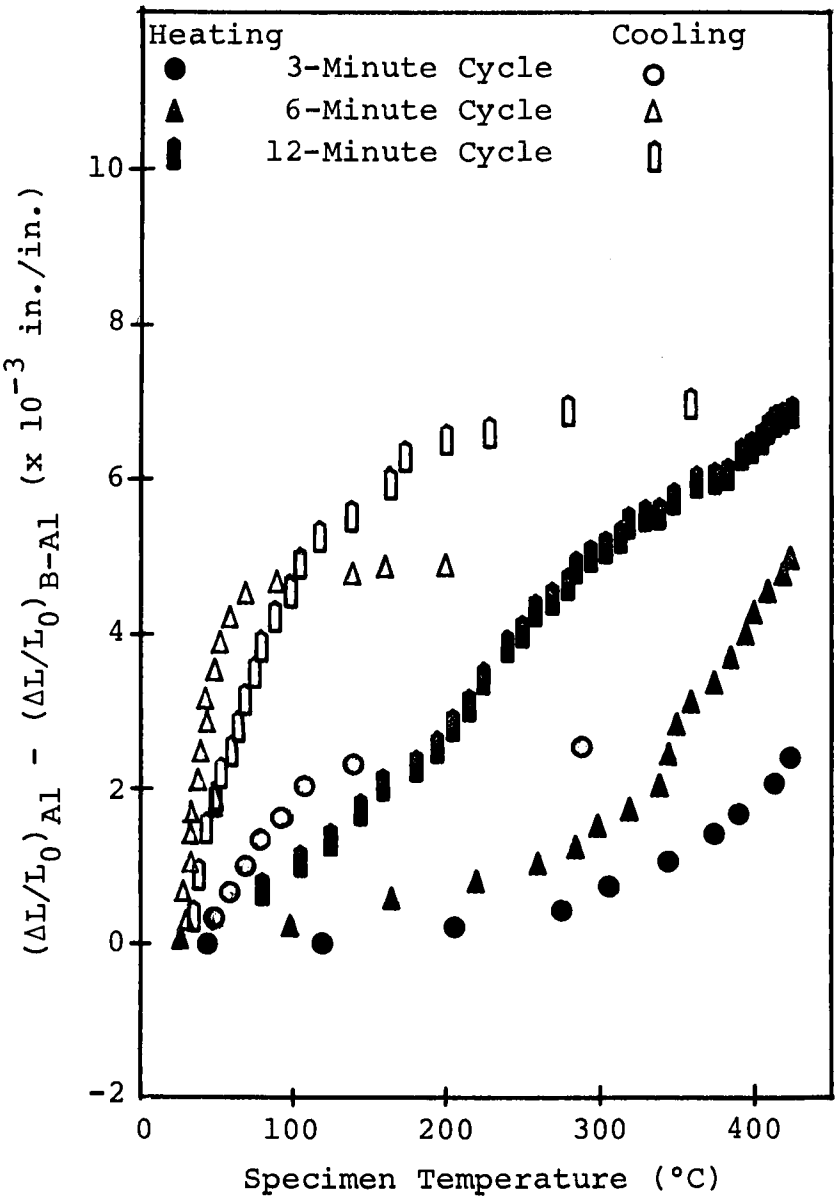

Figure 21. The thermal expansion of boron-aluminum during the four thousandth to forty-ninth hundredth thermal cycles.

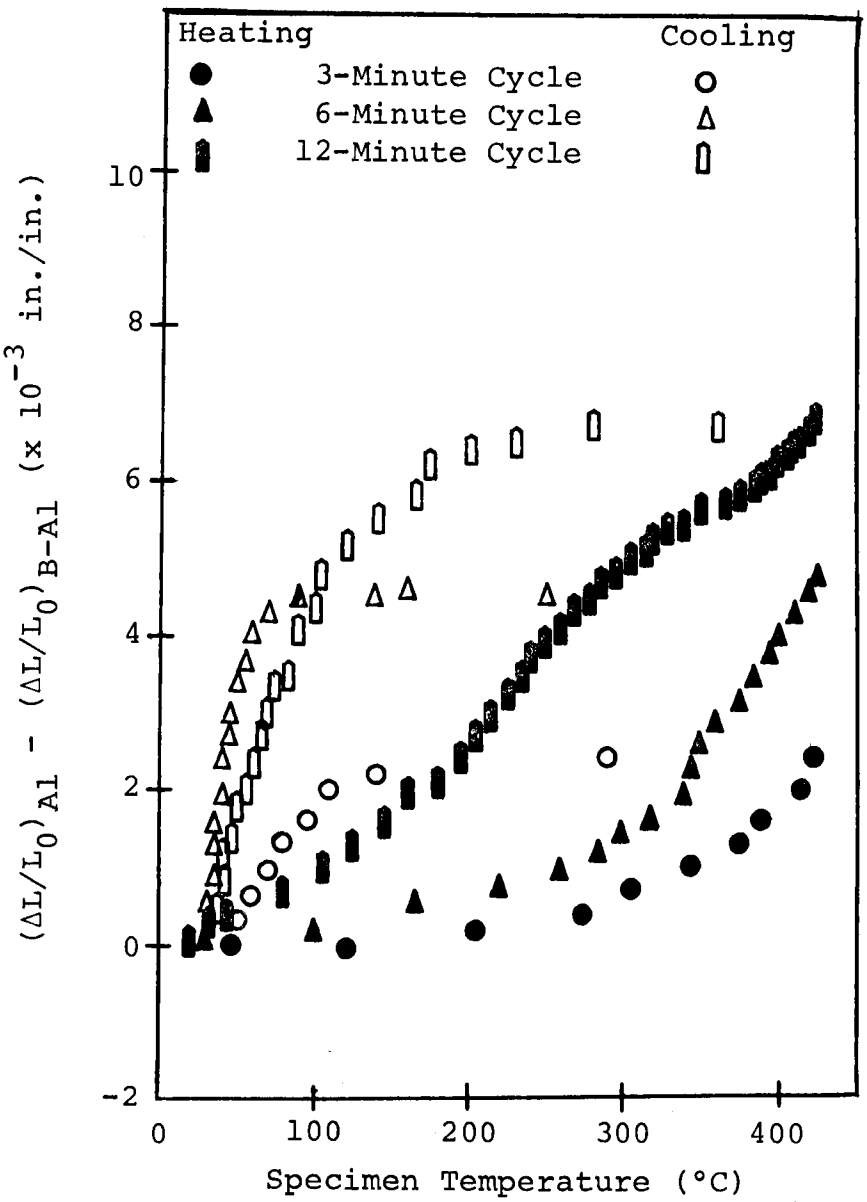

Figure 22. The thermal expansion of boron-aluminum during the six thousandth thermal cycle.

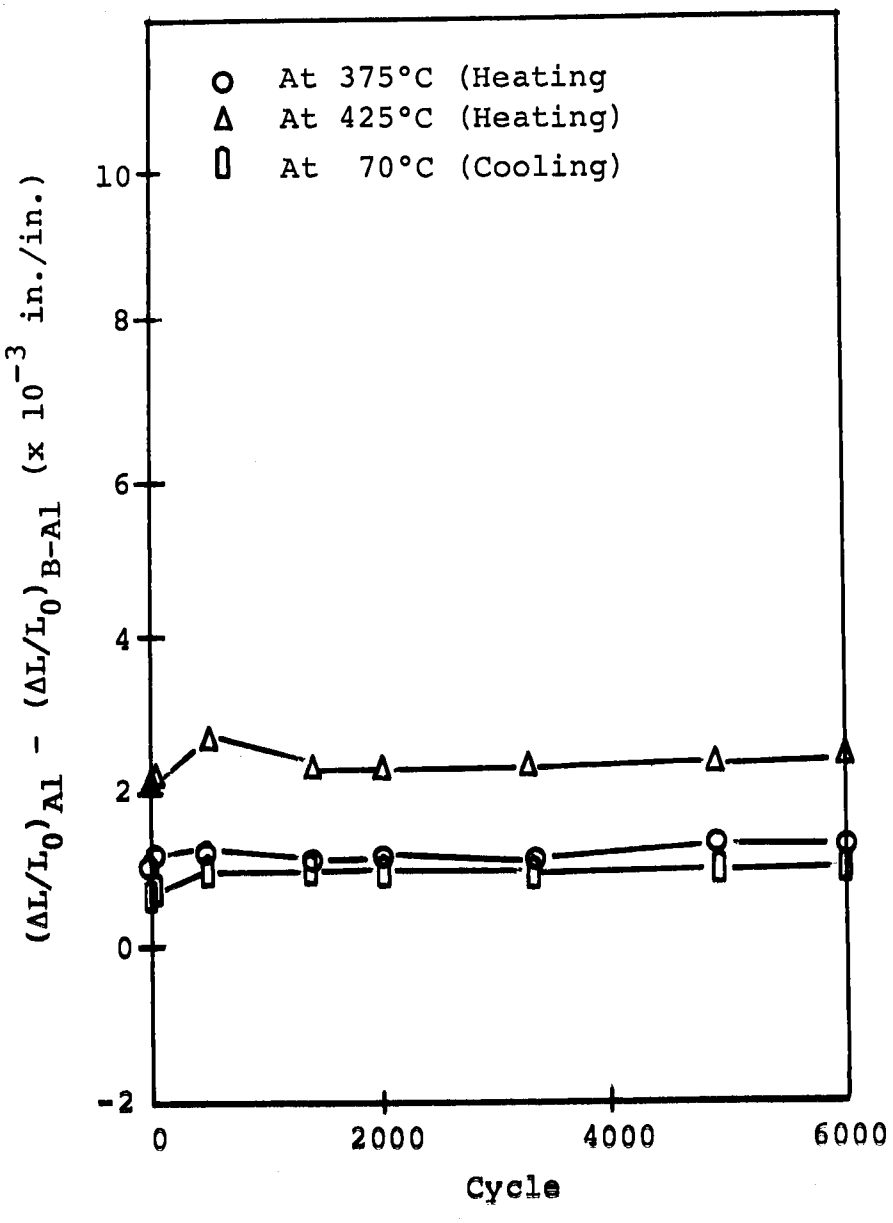

Figure 23. The thermal expansion of boron-aluminum cycled with the three-minute period.

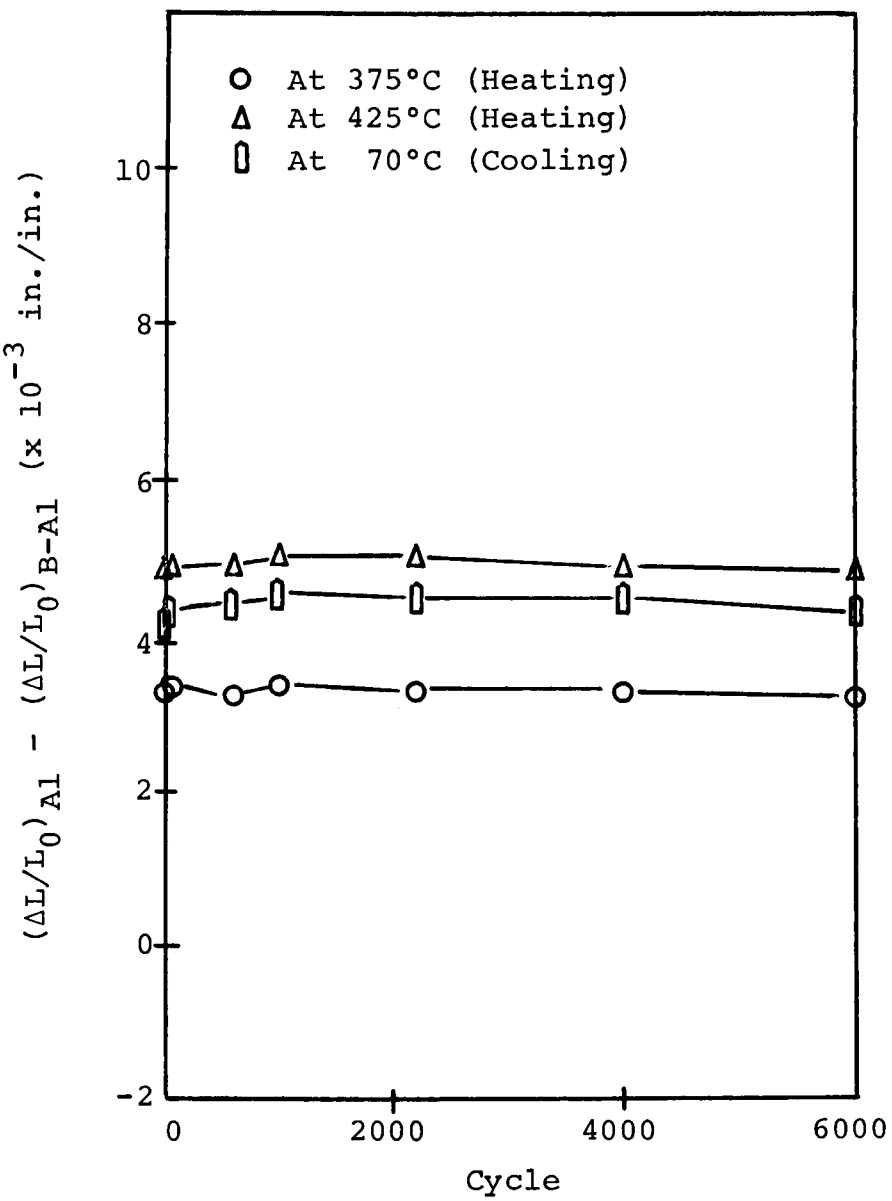

Figure 24. The thermal expansion of boron-aluminum cycled with the six-minute period.

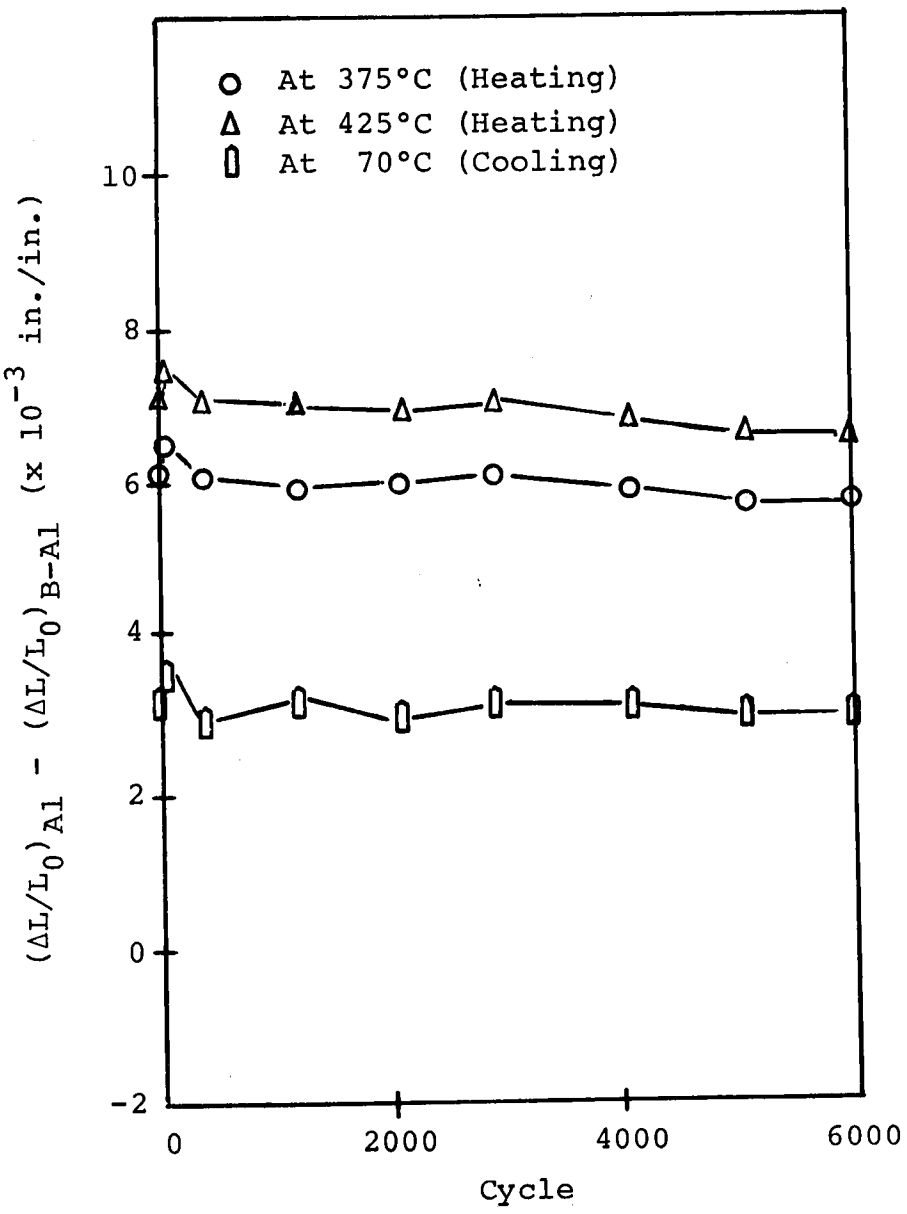

Figure 25. The thermal expansion of boron-aluminum cycled with the twelve-minute period.

VITA

Roy Kyle Holbert, Jr., was born in Asheville, North Carolina on February 27, 1949. He received his preliminary education from schools in Knoxville, Tennessee. He entered Tennessee Technological University where he received a Bachelor of Science degree in Engineering in June, 1972. While attending Tennessee Technological University he worked for nine months as a co-operative student for the Nuclear Division of Union Carbide Corporation. In September, 1972, he accepted a research assistanship at The University of Tennessee Space Institute, and in December, 1975, he was awarded the Master of Science degree in Engineering Science.